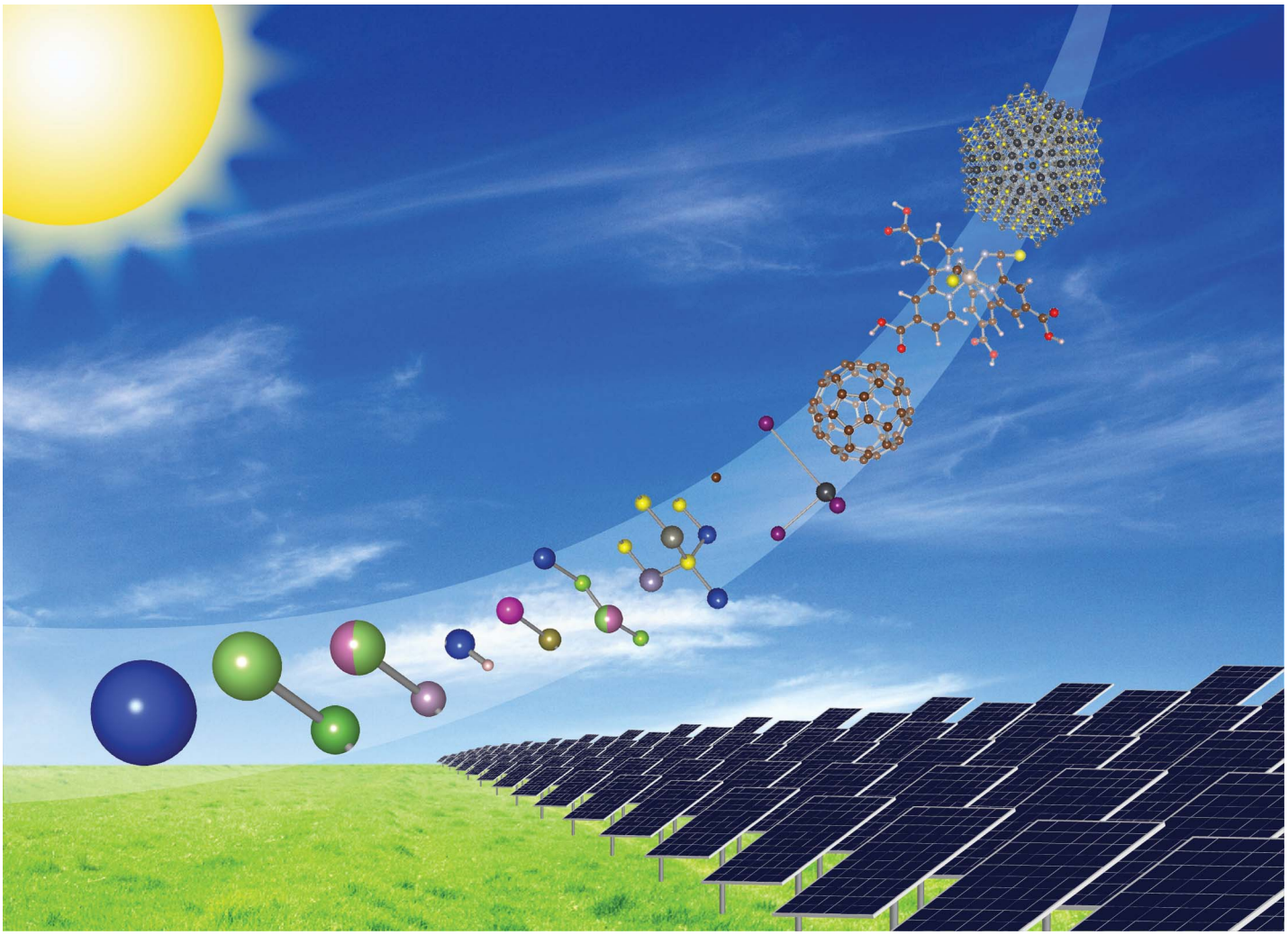

Showcasing research from the group of Professor Vladimir Bulović at the Massachusetts Institute of Technology.

Title: Pathways for solar photovoltaics

Solar photovoltaics (PV) are the fastest-growing energy technology in the world today and a leading candidate for terawatt-scale, carbon-free electricity generation by the mid-century. This Perspective article identifies future technological directions for solar photovoltaics and examines potential limits to PV deployment at the terawatt scale.

As featured in:

See Joel Jean, Vladimir Bulović *et al.*, *Energy Environ. Sci.*, 2015, **8**, 1200.

ROYAL SOCIETY OF CHEMISTRY

www.rsc.org/ees

Registered charity number: 207890

Energy & Environmental Science

PERSPECTIVE

View Article Online
View Journal | View Issue

Cite this: *Energy Environ. Sci.*, 2015, **8**, 1200

Pathways for solar photovoltaics†

Joel Jean,*[a] Patrick R. Brown,[b] Robert L. Jaffe,[bc] Tonio Buonassisi[d] and Vladimir Bulović*[a]

Received 25th December 2014
Accepted 17th February 2015

DOI: 10.1039/c4ee04073b

www.rsc.org/ees

Solar energy is one of the few renewable, low-carbon resources with both the scalability and the technological maturity to meet ever-growing global demand for electricity. Among solar power technologies, solar photovoltaics (PV) are the most widely deployed, providing 0.87% of the world's electricity in 2013 and sustaining a compound annual growth rate in cumulative installed capacity of 43% since 2000. Given the massive scale of deployment needed, this article examines potential limits to PV deployment at the terawatt scale, emphasizing constraints on the use of commodity and PV-critical materials. We propose material complexity as a guiding framework for classifying PV technologies, and we analyze three core themes that focus future research and development: efficiency, materials use, and manufacturing complexity and cost.

Broader context

Solar photovoltaics (PV) are the fastest-growing energy technology in the world today and a leading candidate for terawatt-scale, carbon-free electricity generation by mid-century. Global PV deployment is dominated by crystalline silicon (c-Si) wafer-based technologies, which benefit from high power conversion efficiencies, abundant materials, and proven manufacturability. While PV module costs continue to decline rapidly, however, further system-level cost reductions will likely require lightweight and flexible module designs that are inaccessible with today's c-Si technologies. Various emerging PV technologies promise lower-cost manufacturing and deployment, but none has yet reached large-scale commercial production. In this article, we propose a framework for organizing PV technologies based on material complexity. We review all relevant PV technologies today, analyze their strengths and weaknesses on equal footing, and identify key technological roadblocks to PV deployment at the terawatt scale.

Introduction

Solar photovoltaics (PV) are the most widely deployed solar electric technology today. Fueled by light, solar cells operate near ambient temperature with no moving parts, and they enable distributed generation at any scale: a 10 m^2 PV array is in theory no less efficient per unit area than a 10 km^2 array, unlike thermal generators or wind turbines, which lose efficiency with reduced scale.

In this article, we explore the current status and future trajectory of solar cell technology. After a brief discussion of the solar resource, we review today's PV technologies in three classes: wafer-based, commercial thin-film, and emerging thin-film PV. Key advantages and disadvantages of each technology are discussed. We then introduce a new, unified framework, based on material complexity, for thinking about current and future PV technologies. Within this framework, we identify three primary directions for PV research and development (R&D): efficiency, materials use, and manufacturing complexity and cost. Last, we discuss potential limits on the deployment of solar PV at the terawatt scale, commensurate with international climate-change mitigation targets, with a focus on the cost and availability of commodity and PV-critical materials.

Many of the topics discussed herein have been identified and, in some cases, discussed widely in the literature. However, most previous studies have been concerned primarily with individual technologies or technology classes; few have examined the full range of technologies under investigation today.[1–10] In this work, we analyze all relevant photovoltaic technologies within a single coherent framework. Throughout this article, we assume a baseline familiarity with solar PV. Key background information, including a glossary of terms and a primer on photovoltaics, is presented in the ESI†.

The solar resource

The Sun continuously delivers about 174 000 TW to the upper level of Earth's atmosphere at an average power density of

[a]Department of Electrical Engineering and Computer Science, Massachusetts Institute of Technology, 77 Massachusetts Ave., Cambridge, MA, 02139, USA. E-mail: jjean@alum.mit.edu; bulovic@mit.edu

[b]Department of Physics, Massachusetts Institute of Technology, USA

[c]Center for Theoretical Physics, Massachusetts Institute of Technology, USA

[d]Department of Mechanical Engineering, Massachusetts Institute of Technology, USA

† Electronic supplementary information (ESI) available: Glossary of terms, life cycle carbon intensity analysis, PV fundamentals, and impact of module efficiency on system cost. See DOI: 10.1039/c4ee04073b

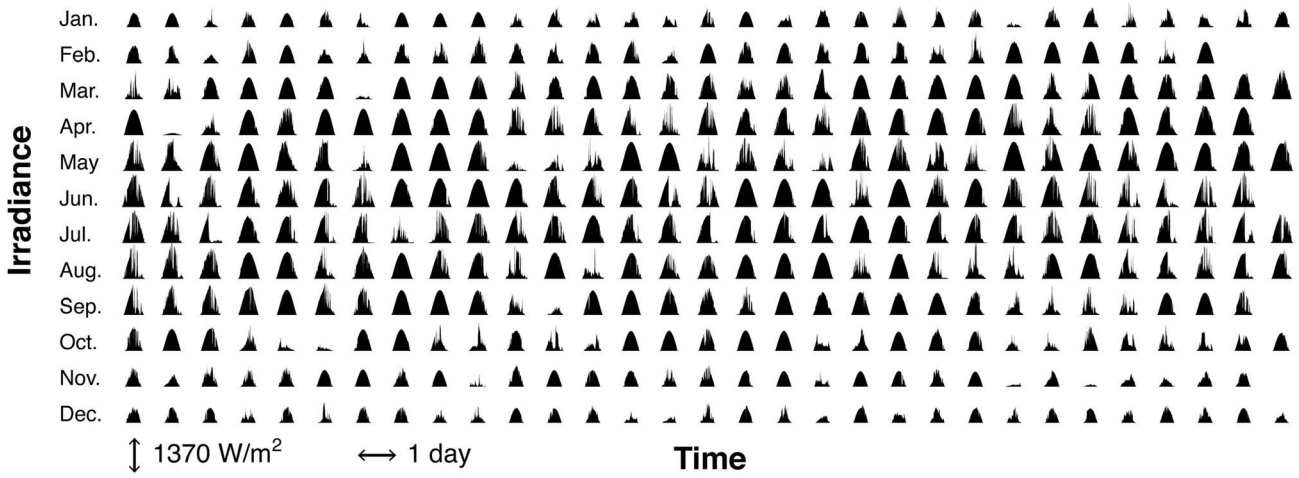

Fig. 1 Complete minute-by-minute solar irradiance profile in Golden, CO, for the year 2012. The time axis is to scale, with nights included. Numerous trends are apparent from these data. The most obvious temporal characteristic of the solar resource is its daily fluctuation. At the shortest timescales, rapid variations arise from shifting cloud cover. On September 1st, for example, the solar intensity drops by a factor of 4 from 12:28–12:30 PM as a result of passing clouds. The month of July is characterized by sharp afternoon reductions in intensity due to frequent afternoon thunderstorms unique to the Colorado Rocky Mountains. Strong day-to-day variations are also observed: the total irradiance delivered on April 1st and 2nd differ by a factor of 15, and some overcast weather systems persist for several days (*e.g.*, October 4–6). Longer variations are also seen over the course of the year. Following a particular day of the month downward, the length of the day as well as the peak and integrated irradiance are seen to increase from winter to summer (January to June) and decrease thereafter.

1366 W m^{-2}, known as the solar constant.‡[11,12] This value is reduced to around 1000 W m^{-2} by atmospheric absorption and scattering, and to between 125 and 305 W m^{-2} (3 to 7.3 kWh per m^2 per day)[13] by latitude-dependent oblique incidence, seasonal variation, and diurnal variation. Ignoring weather-related attenuation, this leaves an annual-average irradiance of roughly 250 W m^{-2} at the average latitude of the continental US (38°N) and of the world's land mass (37°N). Cloud cover and weather further reduce this value to 188 W m^{-2} or 4.5 kWh per m^2 per day in the continental U.S.,[14] comparable to the global-average solar irradiance over land of 183 W m^{-2}.[15] This is our solar budget—the starting point for all solar harvesting technologies.

The solar resource is fundamentally intermittent. An unavoidable challenge for satisfying human energy needs with solar power lies in converting this highly intermittent resource, characterized by dramatic fluctuations in magnitude across wide temporal scales, into a steady and reliable source of electricity.

Intermittency is composed of two types of temporal variation: stochastic and deterministic. Stochastic variability includes the effect of cloud cover and weather, and is inherently unpredictable. Deterministic variability occurs over longer timescales and includes predictable diurnal and seasonal variations as well as local climate. Both types of variation are apparent in Fig. 1, which displays the complete minute-by-minute solar irradiance profile over the year 2012 in Golden, CO.[16] While these data originate from one particular measurement station in one particular year, they illustrate important characteristics of the solar resource that are present at any location in any year. At the shortest timescales of minutes to days, rapid stochastic variations occur from shifting clouds and weather. Longer deterministic variations occur over the course of the year: unsurprisingly, the length of the day as well as the peak and integrated daily irradiance are seen to increase from winter to summer (January to June) and decrease thereafter.

Strategies for managing intermittency differ by time and length scale: local, short-term variation can be smoothed by geographical averaging—power distribution over length scales larger than clouds and weather systems—or by demand management. Managing larger or longer-term variation will require either grid-scale energy storage or deployment of dispatchable or complementary sources.[17]

Despite its temporal and geographical variability, the solar resource remains one of the most equitably distributed energy resources. No location in the world lacks direct local access to sunlight, as shown in Fig. 2. Furthermore, average solar insolation varies by no more than a factor of three across heavily settled areas. Neither of these statements applies to fossil fuels and other extractive energy resources. We also observe that solar availability is not highly correlated with economic wealth. Fig. 2h shows insolation[18] and per-capita GDP in 2011 (ref. 19) for each country for which these data are available. Average insolation is much less variable than GDP, and the weak anti-correlation indicates that developing countries are not fundamentally lacking in access to solar energy. But more importantly, the availability of capital and infrastructure for fully utilizing this resource does vary widely between countries.

‡ The solar constant, defined at a constant distance of 1 AU from the sun, varies slightly—on the order of 0.1%—over the 27-day solar rotation period and the 11-year sunspot cycle.[11] The actual solar irradiance at the Earth's upper atmosphere varies an additional 6.9% annually from perihelion to aphelion due to the Earth's elliptical orbit.[12]

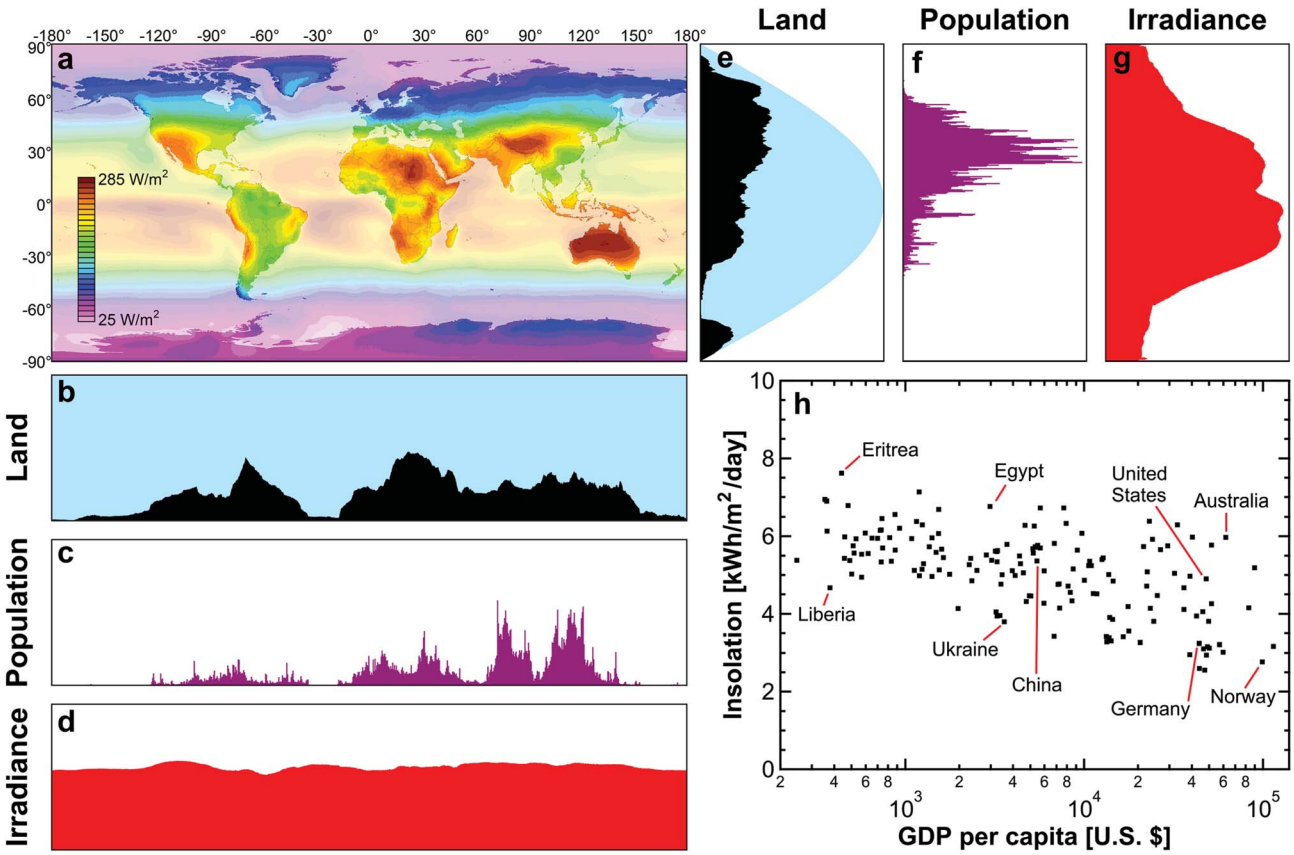

Fig. 2 Worldwide distribution of the solar resource. (a) Global map of solar irradiance [W m^{-2}] averaged from 1990 to 2004 (©Mines ParisTech/Armines 2006).[20] Histograms of world land area [m^2 per °], population [persons per °] (reproduced with permission from ref. 21), and average irradiance at the Earth's surface [W m^{-2}] are shown as a function of longitude (b–d) and latitude (e–g). In (b) and (e), land area is shown in black, and water area is shown in blue. (h) Correlation of average insolation and GDP per capita by country for the year 2011.[18,19] Each dot represents one country.

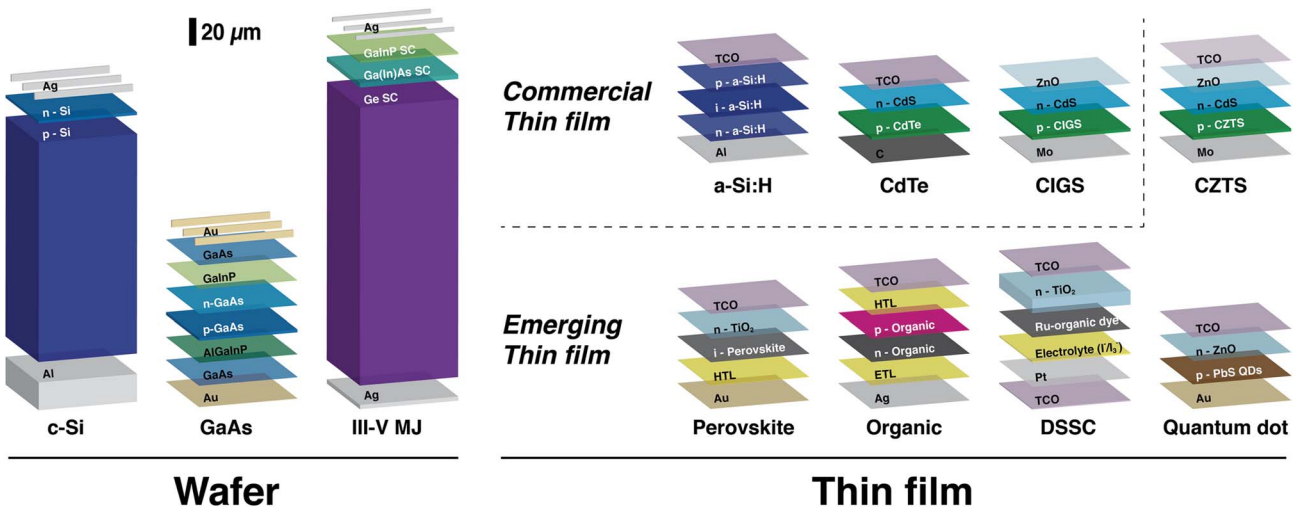

Fig. 3 Typical solar PV device structures, divided into wafer-based and thin-film technologies. Primary absorber layers are labeled in white, and thicknesses are shown to scale. c-Si encompasses sc-Si and mc-Si technologies. GaAs cells use thin absorbing films but require wafers as templates for crystal growth. For III-V multijunctions, sub-cells are shown for the industry-standard GaInP/Ga(In)As/Ge triple-junction cell, and some interface layers are omitted for simplicity. A representative single-junction a-Si:H PV structure is shown here, although PV performance parameters used elsewhere correspond to an a-Si:H/nc-Si:H/nc-Si:H triple-junction cell. Front contact grids are omitted for thin-film technologies since the metals used for those grids do not directly contact the active layers and are thus more fungible than those used for wafer-based technologies.

The PV technology landscape

Solar cell technologies are typically named according to their primary light-absorbing material. As shown in Fig. 3, we can classify PV technologies using two categories: wafer-based and thin-film cells. Wafer-based cells are fabricated on semiconducting wafers and can be handled without an additional substrate, although modules are typically covered with glass for mechanical stability and protection. Thin-film cells consist of semiconducting films deposited onto a glass, plastic, or metal substrate. Here we further divide thin films into commercial and emerging thin-film technologies.

Wafer-based PV

Three primary wafer-based technologies exist today:

• Crystalline silicon (c-Si) solar cells constitute ~90% of current global production capacity and are the most mature of all PV technologies. Silicon solar cells are classified as single-crystalline (sc-Si) or multicrystalline (mc-Si), with respective market shares of ~35% and ~55% in 2014.[22] Cylindrical single crystals are typically grown by Czochralski (CZ)[23,24] or float-zone (FZ) methods, while mc-Si blocks are formed by casting. The resulting ingots are sliced into 150–180 μm wafers prior to cell processing. A high-efficiency sc-Si variant is the heterojunction with intrinsic thin layer (HIT) architecture, which combines *n*-type sc-Si with thin amorphous silicon films, which reduce interface recombination and can increase open-circuit voltages by 5–10%.[25,26] Multicrystalline cells contain randomly oriented grains with sizes of around 1 cm^2. Grain boundaries hinder charge extraction and reduce mc-Si performance relative to sc-Si. Record cell efficiencies stand at 25.6% for sc-Si and 20.8% for mc-Si; large-area module records are 22.4% for sc-Si and 18.5% for mc-Si.[27,28] One fundamental limitation of c-Si is its indirect bandgap, which leads to weak light absorption and requires wafers with thicknesses on the order of 100 μm in the absence of advanced light-trapping strategies. Key technological challenges for c-Si include stringent material purity requirements, high material use, restricted module form factor, and batch-based cell fabrication and module integration processes with relatively low throughput.

○ One emerging research direction for c-Si PV is the use of thin (2–50 μm) c-Si membranes instead of wafers as starting material.[8] Thin films can be produced by thinning of sc-Si wafers,[29,30] epitaxial growth or direct "epi-free" formation on native c-Si substrates with subsequent release and transfer,[31–33] or direct deposition on foreign substrates with a seed layer.[31] Wafer thinning strategies can produce extremely thin (<2 μm) and flexible free-standing silicon layers[29] and have achieved high efficiencies (21.5% with a 47 μm-thick sc-Si wafer[30]), but do not reduce material use or facilitate high-throughput processing. Epitaxial and epi-free transfer approaches have been investigated widely; they allow substrate reuse and can produce high-quality c-Si films and efficient devices with a range of thicknesses (22.3% reported[34] and 21.2% certified cell records[28]). However, epitaxial film growth is relatively slow, and cell areas remain limited to that of conventional wafers. Direct seeded growth on foreign substrates—typically by solid-phase or liquid-phase crystallization[35]—enables high deposition rates and facilitates monolithic integration of durable modules,[36,37] but the resulting polycrystalline films are generally lower in crystallographic quality, leading to lower efficiencies (11.7% reported[35] and 10.5% certified[28] with c-Si on borosilicate glass (CSG)). High-temperature-compatible substrates are also required. Key technical challenges for thin-film c-Si PV include enhancing light absorption by employing advanced anti-reflection and light-trapping strategies, reducing recombination losses by engineering higher-quality crystalline films, reducing processing temperatures to enable flexible substrates and modules without sacrificing material quality, and developing new methods for high-throughput inline module integration.

• Gallium arsenide (GaAs) is almost perfectly suited for solar energy conversion, with strong absorption, a direct bandgap well matched to the solar spectrum, and very low non-radiative energy loss. GaAs has achieved the highest power conversion efficiencies of any material system—28.8% for lab cells and 24.1% for modules.[27,28] A technique known as epitaxial liftoff creates thin, flexible GaAs films and amortizes substrate costs by reusing GaAs wafers,[38] but has not yet been demonstrated in high-volume manufacturing. Cost-effective production will require improved film quality, more substrate reuse cycles, and low-cost wafer polishing, which defines a cost floor for epitaxial substrates. High material costs may limit the large-scale deployment of GaAs technologies.

• III-V multijunction (MJ) solar cells use a stack of two or more single-junction cells with different bandgaps to absorb light efficiently across the solar spectrum by minimizing thermalization losses. Semiconducting compounds of group III (Al, Ga, In) and group V (N, P, As, Sb) elements can form high-quality crystalline films with variable bandgaps, yielding unparalleled power conversion efficiencies—46.0%, 44.4%, and 34.1% for record 4-junction (4J), 3J, and 2J cells, respectively, under concentrated illumination.[27,28] Module records stand at 36.7% and 35.9% for 4J and 3J concentrator modules, respectively.[28] Record cell efficiencies without concentration are 38.8%, 37.9%, and 31.1% for 5J, 3J, and 2J cells, respectively.[27] III-V MJs are the leading technology for space applications, with their high radiation resistance, low temperature sensitivity, and high efficiency. But complex manufacturing processes and high material costs make III-V MJ cells prohibitively expensive for large-area 1-sun terrestrial applications. Concentrating sunlight reduces the required cell area by replacing cells with mirrors or lenses, but it is still unclear whether concentrating PV systems can compete with commercial single-junction technologies on cost. Current R&D efforts are focused on dilute nitrides (*e.g.*, GaInNAs),[39] lattice-mismatched (metamorphic) approaches,[40] and wafer bonding.[41,42] Key challenges for emerging III-V MJ technologies include improving long-term reliability and large-area uniformity, reducing materials use, and optimizing cell architectures for variable operating conditions.

The vast majority of commercial PV module production has been—and is currently—c-Si, for reasons both technical and historical. Silicon can be manufactured into non-toxic, efficient, and extremely reliable solar cells, leveraging the cumulative learning of over 60 years of semiconductor processing for

integrated circuits. Between sc-Si and mc-Si cells, the higher crystal quality in sc-Si cells improves charge extraction and power conversion efficiencies at the expense of more costly wafers (by 20% to 30% (ref. 22)) and material processing. A key disadvantage of c-Si is its relatively poor ability to absorb light, which requires the use of thick, rigid, impurity-free, and expensive wafers. This shortcoming translates to high manufacturing capital costs and constrained module form factors. Despite these limitations, wafer-based c-Si will likely remain the leading deployed PV technology in the near future, and present c-Si technologies could conceivably achieve terawatt-scale deployment by 2050 without major technological advances. Current innovation opportunities include increasing module efficiencies, reducing manufacturing complexity and costs, and reducing reliance on silver for contact metallization.

Solar cells based on thin films of crystalline silicon can potentially bypass key limitations of conventional wafer-based c-Si PV while retaining silicon's many advantages and leveraging existing manufacturing infrastructure. Similarly to commercial thin-film technologies, thin-film c-Si PV can tolerate lower material quality (*i.e.*, smaller grains and higher impurity levels), uses 10–50× less material than wafer-based c-Si PV, may enable lightweight and flexible modules, and allows high-throughput processing. However, efficiencies for high-throughput-compatible approaches remain low compared to both wafer-based and leading commercial thin-film technologies, and manufacturing scalability is unproven. The only thin-film c-Si technology that has been commercialized to date was based on c-Si films on glass, but no companies remain in that market today.

Commercial thin-film PV

While c-Si currently dominates the global PV market, alternative technologies may be able to achieve lower costs in the long run. Solar cells based on thin semiconducting films now constitute ~10% of global PV module production capacity.[22] Thin-film cells are made by additive fabrication processes, which may reduce material usage and manufacturing capital expense. This category extends from commercial technologies based on conventional inorganic semiconductors to emerging technologies based on nanostructured materials.

Key commercial thin-film PV technologies include the following:

• Hydrogenated amorphous silicon (a-Si:H) offers stronger absorption than c-Si, although its larger bandgap (1.7–1.8 eV, compared to 1.12 eV for c-Si) is not well matched to the solar spectrum.[31,43] Amorphous silicon is typically deposited by plasma-enhanced chemical vapor deposition (PECVD) at relatively low substrate temperatures of 150–300 °C. A 300 nm film of a-Si:H can absorb ~90% of above-bandgap photons in a single pass, enabling lightweight and flexible solar cells.[31] Amorphous silicon PV technologies held a global market share of 2% and a thin-film market share of 22% in 2013.[44] An a-Si:H cell can be combined with cells based on nanocrystalline silicon (nc-Si) or amorphous silicon–germanium (a-SiGe) alloys to form a multijunction cell without lattice-matching requirements. Most commercial a-Si:H modules today use multijunction cells. Silicon is cheap, abundant, and non-toxic, but while a-Si:H cells are well suited for small-scale and low-power applications, their susceptibility to light-induced degradation (the Staebler–Wronski effect[45]) and their low efficiency compared to other mature thin-film technologies (13.4% triple-junction cell record and 12.2% dual-junction module record[27,28]) limit market adoption.

• Cadmium telluride (CdTe) is the leading thin-film PV technology, with a global PV market share of 5% and a thin-film market share of 56% in 2013.[44] CdTe is a favorable semiconductor for solar energy harvesting, with strong absorption across the solar spectrum and a direct bandgap of 1.45 eV.[31] Record efficiencies of 21.0% for cells and 17.5% for modules[27,28] are among the highest for thin-film solar cells, and commercial module efficiencies continue to improve steadily. CdTe technologies employ high-throughput deposition processes and offer the lowest module costs of any PV technology on the market today, although relatively high processing temperatures are required (~500 °C). Concerns about the toxicity of elemental cadmium[46] and the scarcity of tellurium have motivated research on alternative material systems that exhibit similar ease of manufacturing but rely on abundant and non-toxic elements.

• Copper indium gallium diselenide ($CuIn_xGa_{1-x}Se_2$, or CIGS) is a compound semiconductor with a direct bandgap of 1.1–1.2 eV. CIGS technologies held a global PV market share of 2% and a thin-film market share of 22% in 2013.[44] Like CdTe, CIGS films can be deposited by a variety of solution- and vapor-phase techniques on flexible metal or polyimide substrates,[47] favorable for building-integrated and other unconventional PV applications. CIGS solar cells exhibit high radiation resistance, a necessary property for space applications. Record efficiencies stand at 21.7% for cells and 17.5% for modules.[27,28] Key technological challenges include high variability in film stoichiometry and properties, limited understanding of the role of grain boundaries,[48] low open-circuit voltage due to structural and electronic inhomogeneity,[49] and engineering of higher-bandgap alloys to enable multijunction devices.[31,50] Scarcity of indium could hinder large-scale deployment of CIGS technologies.

The active materials used in commercial thin-film PV technologies absorb light 10–100 times more efficiently than silicon, allowing use of films just a few microns thick. Low materials use is thus a key advantage of these technologies. Advanced factories can produce thin-film modules in a highly streamlined and automated fashion. Furthermore, life cycle analyses suggest that thin films produce lower greenhouse gas emissions during production and use than c-Si PV (45 g CO_2-eq per kWh for c-Si,[51] compared to 21, 14, and 27 g CO_2-eq per kWh for a-Si:H, CdTe, and CIGS, respectively[52]).§

§ The life cycle carbon footprint of solar PV (in g CO_2-eq per kWh) is dominated by emissions from energy consumption during materials processing and module manufacturing. It has been suggested that the manufacturing of PV modules in countries with a high carbon intensity of electricity and subsequent deployment in countries with lower carbon intensities may diminish the low-carbon benefits of solar PV. We analyze this effect in the ESI† and conclude that if the goal is to reduce emissions, it is far less important where PV is manufactured than where it is deployed, and most important whether it is deployed at all.

A key disadvantage of today's commercial thin-film modules is the comparatively low average efficiencies of 12–15%, compared to 15–21% for c-Si. Low efficiencies increase system costs due to area-dependent balance-of-system (BOS) costs such as wiring and mounting hardware. Most thin-film materials today are polycrystalline and contain much higher defect densities than c-Si. Some compound semiconductors such as CIGS have complex stoichiometry, making high-yield, uniform, large-area deposition a formidable process-engineering challenge. Sensitivity to moisture and oxygen often requires more expensive hermetic encapsulation to ensure 25-year reliability. Use of regulated, toxic elements (*e.g.*, Cd) and reliance on rare elements (*e.g.*, Te, In) may limit the potential for large-scale deployment. Current innovation opportunities in thin films include improving module efficiency, improving reliability by introducing more robust materials and cell architectures, and decreasing reliance on rare elements by developing new materials with similar ease of processing.

Emerging thin-film PV

In recent years, several new thin-film PV technologies have emerged as a result of intense R&D efforts in materials discovery and device engineering. Key emerging thin-film PV technologies include the following:

• Copper zinc tin sulfide (Cu_2ZnSnS_4, or CZTS) is an Earth-abundant alternative to CIGS, with similar processing strategies and challenges.[53,54] One key challenge involves managing a class of defects known as cation disorder: uncontrolled inter-substitution of Cu and Zn cations creates point defects that can hinder charge extraction and reduce the open-circuit voltage.[55] Record certified cell efficiencies have reached 12.6%.[28,56]

• Perovskite solar cells evolved from solid-state dye-sensitized cells[57,58] and have quickly become one of the most promising emerging thin-film PV technologies, with leading certified efficiencies reaching 20.1% (ref. 27 and 28) in less than 3 years of development.[59–61] The term "perovskite" refers to the ABX_3 crystal structure, and the most widely investigated perovskite for solar cells is the hybrid organic–inorganic lead halide $CH_3NH_3Pb(I,Cl,Br)_3$. Optical bandgaps can be tuned from ~1.25 to 3.0 eV by cation (A, B) or anion (X) substitution (*e.g.*, $HC(NH_2)_2Pb(I_{1-x}Br_x)_3$,[62] $CH_3NH_3SnI_3$,[63,64] and $CH_3NH_3Pb(I_{1-x}Br_x)_3$ (ref. 65)). Polycrystalline films can be formed at low temperatures by solution or vapor deposition.[66–68] Key advantages of this class of material include long carrier diffusion lengths,[69,70] low recombination losses,[71] low materials cost, and bandgap tunability. Early perovskite devices have achieved high open-circuit voltages (>1.1 V), typically the most difficult PV performance parameter to improve. Key challenges include refined control of film morphology and material properties, high sensitivity to moisture, unproven cell stability, and the use of toxic lead.[59,60]

• Organic photovoltaics (OPV) use organic small molecules[72,73] or polymers[74–76] to absorb light.[77–80] These materials consist mostly of Earth-abundant elements and can be assembled into thin films by large-area, high-throughput deposition methods.[81] Organic multijunction cells may be much easier to fabricate than conventional III-V MJs because of their high defect tolerance and ease of deposition.[82] Small-molecule and polymer OPV cells have reached 11.1% certified efficiencies, with module efficiencies reaching 8.7%.[27,28] Key concerns involve inefficient exciton transport,[72,74,76] poor long-term stability,[83] low large-area deposition yield, and low ultimate efficiency limits.[84]

• Dye-sensitized solar cells (DSSCs) are among the most mature of nanomaterial-based PV technologies.[85–87] These photoelectrochemical cells consist of a transparent inorganic scaffold anode (typically nanoporous TiO_2) sensitized with light-absorbing dye molecules (usually ruthenium (Ru) complexes).[88,89] Unlike the other solid-state technologies discussed here, DSSCs often use a liquid electrolyte to transport ions to a counter electrode, although efficient solid-state devices have also been demonstrated.[86,90,91] DSSCs have achieved efficiencies of up to 12.3% (ref. 92) (11.9% and 8.8% certified cell and module records, respectively[27,28]) and may benefit from low-cost materials, simple assembly, and colorful and flexible modules. Key challenges involve limited long-term stability under illumination and high temperatures, low absorption in the near-infrared, and low open-circuit voltages caused by interfacial recombination.[31]

• Colloidal quantum dot photovoltaics (QDPV) use solution-processed nanocrystals, also known as quantum dots (QDs), to absorb light.[93–98] The ability to tune the bandgap of colloidal metal chalcogenide nanocrystals (primarily PbS) by changing their size allows efficient harvesting of near-infrared photons, as well as the potential for multijunction cells using a single material system.[99,100] QDPV technologies are improving consistently, with a record certified cell efficiency of 9.2%,[27] and they offer simple room-temperature fabrication and air-stable operation.[101] Key challenges include incomplete understanding of QD surface chemistry[102–105] and low open-circuit voltages that may be limited fundamentally by mid-gap states or inherent disorder in QD films.[106,107]

These emerging thin-film technologies employ nanostructured materials that can be engineered to achieve desired optical and electronic properties. Reliance on Earth-abundant materials and relatively simple processing methods bodes well for large-scale manufacturing and deployment. While these technologies range in maturity from fundamental materials R&D to early commercialization and have not yet been deployed at scale, they offer potentially unique device-level properties such as visible transparency, high weight-specific power [W g^{-1}], and flexible form factors. These qualities could open the door to novel applications for solar PV. In the long term, emerging thin-film technologies may overcome many of the limitations of today's deployed technologies at low cost, assuming improvements in efficiency and stability are realized.

PV technology classification by material complexity

Historical "generation"-based classification

Solar PV technologies can be ranked by power conversion efficiency (PCE), module cost, material abundance, or any other performance metric. The most widely used classification scheme today focuses on two metrics, module efficiency and

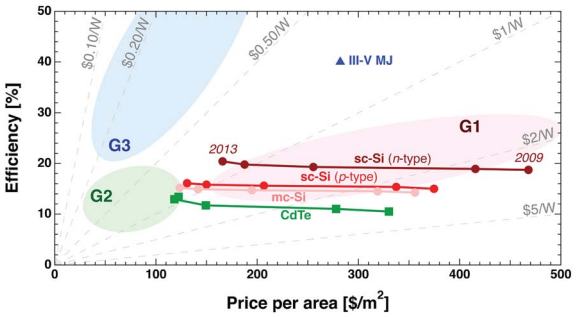

Fig. 4 Limited utility of generational classification scheme. Average module efficiencies[108] and price per area[109] from 2009–2013 are shown for commercial PV technologies in three conventional generations (G1 in red, G2 in green, and G3 in blue). Most current G1 and G2 modules cluster near the region originally defined as G2. The single G3 data point corresponds to performance projections for a III-V MJ module.[42]

area cost, that delineate the three distinct generations listed below.[6,7,10]

(1) First-generation (G1) technologies consist of wafer-based cells of c-Si and GaAs.

(2) Second-generation (G2) technologies consist of thin-film cells, including a-Si:H, CdTe, and CIGS.

(3) Third-generation (G3) technologies include novel thin-film devices, such as dye-sensitized, organic, and quantum dot solar cells, along with a variety of "exotic" concepts, including spectral-splitting devices (*e.g.*, multijunction cells), hot-carrier collection, carrier multiplication, and thermophotovoltaics.[6,7,31]

This generational scheme may not adequately describe the modern PV technology landscape. Emerging technologies like QD and perovskite solar cells have largely been lumped together under the third-generation label of "advanced thin films".[10] Furthermore, any chronological classification scheme is likely to treat older technologies pejoratively in favor of new "next-generation" concepts, even as silicon and commercial thin-film technologies far outperform today's emerging thin-film technologies.

The three generations are commonly represented as shaded regions on a plot of efficiency *vs.* area cost. Fig. 4 shows these regions as originally defined in 2001,¶[6] along with module performance trends for commercial PV technologies from 2009–2013.[108,109] All technologies move toward the upper-left corner with time as efficiencies rise and costs fall. Current modules do not fall in the marked zones. Nearly all current G1 and G2 technologies appear close to the zone designated G2. Furthermore, no third-generation technology to our knowledge has reached the zone marked G3. More generally, we find that average commercial module prices for both G1 and G2 tend to cluster along a single \$ per W_p line in any given year, likely due to competitive market dynamics.

Complexity-based classification

We propose an alternative approach to PV technology classification based on material complexity that we have found useful. Material complexity can be defined roughly as the number of atoms in a unit cell, molecule, or other repeating unit.‖ The repeating units that constitute the active material in modern PV technologies run the gamut in complexity from single silicon atoms to QDs containing thousands of lead and sulfur atoms.

In this framework, all PV technologies fall on a spectrum from elemental (lowest) to nanomaterial (highest) complexity, shown in Fig. 5. At one end of the material complexity spectrum are wafer-based technologies with relatively simple building blocks, including c-Si and III-V cells. Technologies based on more complex materials fall under the broad umbrella of thin-film solar cells, ranging from polycrystalline thin films such as CdTe and CIGS to complex nanomaterials such as organics and QDs.

Material complexity is not equivalent to processing complexity. In fact, one is often traded for the other: silicon may be considered a simple material, but processing it is a complex industrial procedure due to relatively stringent purity requirements.** More complex materials typically employ solution-based synthetic procedures. Once synthesized, these materials can be deposited as thin films quickly and easily, without expensive equipment or high-temperature processing.

We note that higher material complexity is not always "better". Technological maturity and cell efficiencies tend to vary inversely with complexity. In the history of semiconductor technology, bulk crystalline materials based on elemental and compound building blocks were discovered, studied, and engineered first, for electronic and optoelectronic devices alike. The first solar cell, made in 1883 by Charles Fritts, was based on a wafer of selenium. Less-complex materials like silicon are better understood than novel nanomaterials, and improved control over electronic and optical properties allows better device modeling and engineering. Silicon and conventional III-V semiconductors have achieved the highest efficiencies among PV technologies. Indeed, silicon now commands the vast majority of the global market.

Increased material complexity, however, does give rise to several novel attributes of value:

¶ The generations shown in Fig. 4 are typically represented in terms of cost per area, rather than price per area. Here we use module prices because manufacturing cost data are not consistently available. However, we must emphasize that price is an imperfect proxy for underlying costs. Reductions in module price do not always reflect technological progress.

‖ Material complexity is associated with the degree of disorder in a material. Amorphous materials can be qualitatively classified as generally more complex than their crystalline counterparts, since relative atomic positions are well defined in crystals, less so in polycrystalline films, and not at all in amorphous films.

** Solar-grade silicon is typically refined to a purity of "six nines" (99.9999%). Integrated circuit manufacturing requires a silicon purity of "nine nines" (99.9999999%). For comparison, materials used in organic solar cells and other emerging thin-film technologies often have measurable purities on the order of 99%; less-stringent purity requirements often reduce processing complexity and cost.

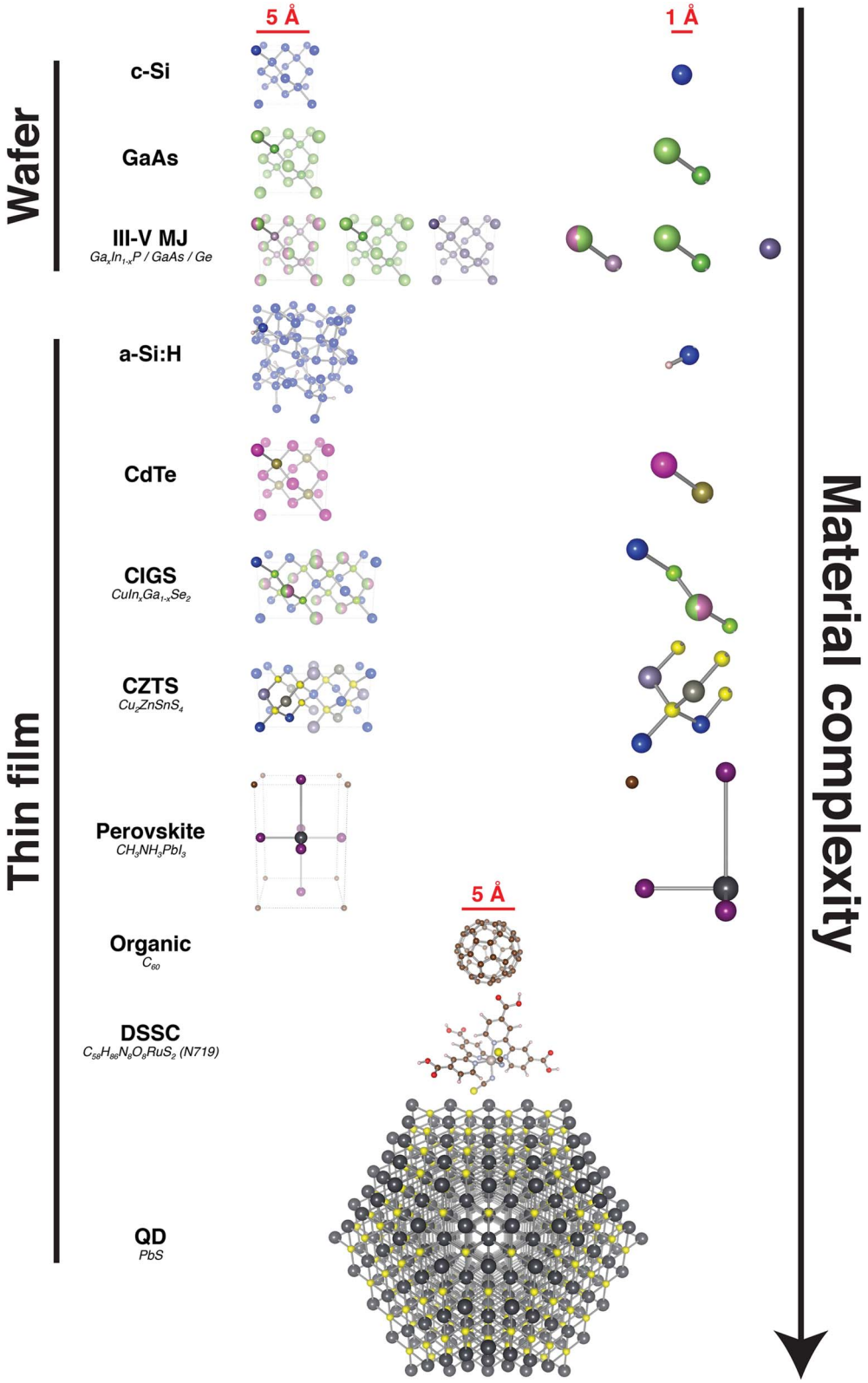

Fig. 5 Alternative PV technology classification scheme based on material complexity. Crystal unit cells or molecular structures of representative materials are shown for each technology, with crystal bases highlighted and expanded (right column) to illustrate the relative complexity of different material systems. Wafer-based materials consist of single- or few-atom building blocks. Thin-film materials range from amorphous elemental materials (a-Si:H) to complex nanomaterials with building blocks containing up to thousands of atoms (*e.g.*, PbS QDs). Lattice constants and bond lengths are shown to scale, while atomic radii are 40% of actual values in comparison. Single carbon atoms (brown) in the perovskite crystal structure represent methylammonium (CH_3NH_3) cations.

Reduced materials use. Absorber thicknesses tend to decrease with increasing complexity, since complex building blocks are often engineered or selected for maximum light absorption. Strong absorption in nanomaterials reduces material use and cell weight.

Improved defect tolerance. Crystallographic defects, non-stoichiometry, and impurities tend to hinder exciton and carrier transport and limit PV performance. Thinner active layers reduce the distance traveled by photogenerated charges and thus increase defect tolerance. In general, complex nanomaterials may tolerate imperfections more readily than single-crystalline and polycrystalline materials.

Flexible substrates and versatile form factors. Commercial thin-film PV technologies are characterized by one-step formation of the absorber material on a substrate, while emerging thin films often employ separate active material synthesis and deposition steps. Building blocks such as organic molecules and QDs can be synthesized in a separate chemical reaction at high temperatures and deposited at low temperatures. Flexible and lightweight substrates (*e.g.*, plastic[110,111] or paper[112]) can then be used, potentially enabling high specific power.

Visible transparency. The lack of long-range crystalline order in organic molecules leads to light absorption that does not strictly increase with photon energy. Non-monotonic absorption allows some organic materials to absorb infrared radiation while transmitting visible light, potentially enabling the development of visibly transparent solar cells.[113,114]

Future solar cell applications may well require some or all of these performance characteristics, and improving the conversion efficiency and stability of these complex material platforms is a key priority for PV technology development.

Performance metrics for future PV applications

To understand the challenges facing PV technology adoption, it is instructive to define performance metrics by which candidate PV technologies can be compared. These metrics may be purely technical or may incorporate both technical and economic factors. Here we consider key metrics driving adoption in two primary classes of PV applications: grid connected and off grid.

Grid-connected applications employ ground- or roof-mounted PV arrays at the residential (peak power output $\leq$ 10 kW_p), commercial (10 kW_p to 1 MW_p), or utility (>1 MW_p) scale. Grid connectivity imposes a single dominant requirement: low levelized cost of energy (LCOE, in $ per kWh). A comparison of LCOE for solar PV and for competing generation sources dictates the economic feasibility of a grid-connected PV system. Recent analysis suggests that the current LCOE for unsubsidized PV in the U.S. ranges from roughly $0.11 per kWh to $0.16 per kWh for utility-scale systems and from $0.19 per kWh to $0.29 per kWh for residential systems.[13] Federal tax subsidies reduce these values by 20–40%, depending on the effectiveness of the subsidy, to $0.07 per kWh to $0.13 per kWh for utility-scale systems and $0.12 per kWh to $0.23 per kWh for residential systems.††

However, LCOE alone may underestimate the value of solar generation due to temporal variation in electricity demand and price.[115] Other important metrics include system cost ($ per W_p), reliability, and where roof loading is crucial, specific power. All but the last of these directly affect LCOE.

It is worth noting the growing importance of non-module costs in grid-connected PV system cost. Since the year 2000, average system prices in the U.S. have decreased by over 50%.[116] Current average system costs in the U.S. are estimated at roughly $3.25 per W_p for residential and $1.80 per W_p for utility-scale systems.[13] But these reductions have been primarily due to falling module prices. BOS costs, which include auxiliary hardware (*e.g.*, inverters, wiring, and racking) as well as installation labor, customer acquisition, permitting, inspection, interconnection, sales tax, and financing, have remained relatively constant and now constitute up to 80% of residential and 60% of utility-scale system cost in the U.S.[13] In Germany, arguably a more mature market, the ratio between module and BOS is closer to 50/50. An important present R&D theme is thus new materials, processes, and designs that can substantially lower BOS costs.

Off-grid applications, including portable devices and deployment in developing countries, tend to value system cost along with a variety of non-cost factors, such as specific power, form factor (*e.g.*, flexibility), aesthetics, and durability. One example is the use of small-area solar cells to power mobile phones, small water purification systems, and other portable electronic devices. In many applications, significant value may derive from low module weight. We note that PV technologies with lifetimes too short or efficiencies too low to power today's high-power mobile devices may be adequate for the low-power lighting and communication requirements of the developing world.

Another potential off-grid application is building-integrated PV (BIPV), the use of PV modules in structural features whose primary purpose is *not* electricity generation (*e.g.*, windows, skylights, shingles, tiles, curtains, and canopies). Aesthetic concerns often drive module form factor and positioning, which may be sub-optimal for solar energy collection. That said, some BIPV systems may achieve competitive LCOE by piggybacking on the materials, installation, and maintenance costs of the existing building envelope. Other potential application areas for PV are discussed below.

Fig. 6 compares the technological maturity, power conversion efficiency, and specific power of today's PV technologies ordered by material complexity. We make several observations: (1) Crystalline silicon and conventional thin films are the only technologies deployed at large scale today. (2) Record module

†† Current federal tax preferences for solar energy include a 30% investment tax credit (ITC) and a 5-year accelerated depreciation schedule. Various other energy technologies—*e.g.*, fuel cells, small wind turbines, geothermal, and combined heat and power (CHP) systems—also qualify for similar tax benefits.

efficiencies lag behind lab-cell efficiencies by a significant margin. (3) Thin-film PV technologies use 10 to 1000 times less material than c-Si, reducing cell weight per unit area and increasing power output per unit weight. (4) All deployed PV technologies have been under development for at least three decades.

Unique PV applications

The technical demands of diverse applications will continue to drive major foundational R&D effort toward the development of alternative PV technologies. These technologies can be classified according to their purpose:

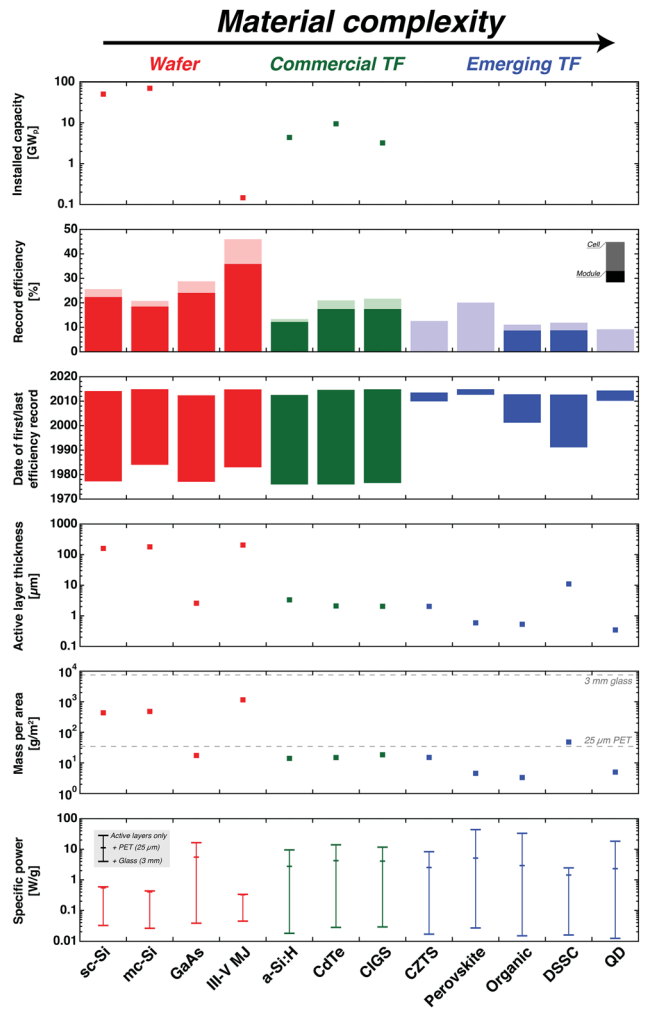

Fig. 6 Key metrics, at the time of this writing, for PV technologies ordered by increasing material complexity. Cumulative global installed capacity,[44,129] power conversion efficiency under 1 sun (except III-V MJ), time elapsed since first NREL certification, absorber thickness, and cell mass per area all generally decrease with increasing material complexity. Specific power is shown for active layers alone and for cells with a 25 μm polyethylene terephthalate (PET) or 3 mm glass substrate or encapsulation layer. Specific power is calculated for III-V MJs based on the record cell efficiency under 1 sun (38.8%). Despite their lower efficiencies, thin-film cells on thin and flexible substrates can achieve much higher specific power than wafer-based cells.

Ultra-high efficiency. Some applications (*e.g.*, satellites and defense applications) require efficiencies over 30%, twice that of typical commercial modules. Achieving such high efficiencies typically requires more expensive approaches involving multiple absorber materials (*e.g.*, multijunction and spectral-splitting devices) or solar concentration. Recently, substantial R&D effort has focused on combining c-Si technology with an overlayer of wide-bandgap thin-film material,[117] such as III-Vs, chalcogenides, metal oxides, or perovskites.[60]

Unique form factors. Some applications may benefit from form factors that depart from traditional glass-covered modules. Examples include BIPV, portable consumer devices, and solar textiles.

Unique aesthetics. Colored or transparent solar cells, which absorb primarily infrared or ultraviolet light, may be considered to have aesthetic advantages when incorporated into certain applications, including construction façades, windows, and consumer electronics.

Measuring PV module and system performance

In a deployed PV system, energy output does not depend on the rated efficiency alone. The DC peak power rating of a PV module or system (in W_p) reflects its efficiency under standard test conditions (STC): 1000 W m^{-2} irradiance, 25 °C operating temperature, and Air Mass 1.5 (AM1.5) spectrum. But the actual AC energy output depends strongly on local insolation, shading losses (*e.g.*, soiling and snow coverage), module efficiency losses (*e.g.*, due to elevated temperatures, low irradiance, or increased reflection at non-normal incidence), and system losses (*e.g.*, module mismatch, wire resistance, inverter and transformer losses, tracking inaccuracy, and age-related degradation). For example, a PV module that maintains its rated efficiency at low light levels could produce more power over the course of a day than a module with the same power rating but reduced efficiency under low irradiance (*e.g.*, during evening hours).

An important performance metric is thus energy yield (kWh/kW$_p$), which is directly related to system-level metrics such as capacity factor and performance ratio, as discussed below. Energy yield quantifies the AC energy output per unit of installed capacity. To reduce LCOE, module and BOS technology development will attempt to increase energy yield, making heat and light management, durability, and reliability more important. An inherent tension exists between improving these technical factors and reducing area costs. Identifying key operating parameters that affect energy yield for different technologies is a critical research priority.

The performance of a deployed PV system is typically characterized by its actual AC energy output per year, relative to the expected DC output. The expected output can be calculated in terms of either ideal or actual insolation, yielding two different metrics. The capacity factor (CF) compares system output to the performance of an ideal (lossless) system with identical nameplate capacity operating at 25 °C under constant peak

($1000\ \mathrm{W\ m^{-2}}$) irradiance. The performance ratio (PR) or quality factor (Q) instead compares system output to that of an ideal system operating at 25 °C in the same location (*i.e.*, under local insolation).

$$\mathrm{CF} = \frac{\text{Actual AC energy output [kWh per year]}}{\text{DC peak power rating } [\mathrm{kW_p}] \times 8760[\text{h per year}]}$$

$$\mathrm{PR} = \frac{\text{Actual AC energy output [kWh per year]}}{\text{DC peak power rating } [\mathrm{kW_p}] \times 8760[\text{h per year}] \times \dfrac{\text{Average plane-of-array irradiance } [\mathrm{W\ m^{-2}}]}{1000[\mathrm{W\ m^{-2}}]}}$$

Capacity factors are commonly used to compare power generation systems. The annual capacity factor for a typical utility-scale solar PV system in the U.S. is around 20%, compared to 22% for solar thermal, 31% for wind, 40% for hydropower, 44% for natural gas combined cycle, 64% for coal, and 90% for nuclear power plants.[118] Solar power systems without storage can operate only when sunlight is available; this constraint alone limits the capacity factor to the fraction of daylight hours. By accounting for geographical and temporal variations in insolation, the performance ratio isolates non-ideal module and system losses (*e.g.*, due to elevated temperatures or component failures) and allows comparison of PV systems in different locations. Typical performance ratios range from 60% to 90%.

PV R&D pathways

The performance metrics described above reflect application-specific performance demands. The extent to which these needs are fulfilled by any particular PV technology will determine the commercial viability of that technology. These metrics lead us to three key themes common to PV technology development: efficiency, materials use, and manufacturing complexity and cost. Technologies that excel in each of these categories are suitable for deployment in a wide variety of applications. In this section we discuss R&D strategies and priorities across these themes.

Power conversion efficiency (PCE) [% or W $\mathrm{m^{-2}}$]

Increasing power conversion efficiency has traditionally been the target of major PV R&D efforts. While we have stressed the importance of alternative performance metrics, new technologies must nonetheless reach a minimum PCE to be economically feasible for most applications. Fig. S11 in the ESI† illustrates the effect of module efficiency on system costs. Efficient cells and modules reduce system costs per peak watt, since some BOS components scale with module area. These area-dependent BOS costs dominate the total system cost when module efficiencies are low. Research efforts should thus target PV technologies that have demonstrated potential to reach high (>15%) efficiencies. Key technological approaches to boosting cell efficiency include improving surface passivation to reduce recombination loss, identifying more conductive transparent electrode materials to reduce resistive losses,[119,120] engineering optical and electronic materials to improve current collection, and employing advanced cell architectures.

Solar PV efficiency is fundamentally restricted to the Shockley–Queisser limit of ~33.7% for single-junction cells operating at 300 K under the AM1.5G spectrum.[121–123] For mature technologies—*i.e.*, those approaching their limiting efficiencies—little room for improvement remains. In such cases, material use and processing innovations should be prioritized over cell efficiency gains.

Complementing the need for high efficiency is the need for maintaining high efficiencies stably over the lifetime required for a given application. For most applications, a 15%-efficient solar cell that operates reliably for 25 years is more valuable than a 25%-efficient cell that degrades completely within months.‡‡ However, initial high efficiency is a prerequisite for maintaining high efficiency over time, so efficiency improvements should be prioritized over lifetime studies for emerging technologies. Research toward improving reliability and lifetime includes investigations of air-stable and water-insensitive materials, light- or moisture-induced degradation mechanisms, and barrier and encapsulation layers.

Module *vs.* cell efficiency

Module PCEs tend to approach cell PCEs with increasing development time, highlighting the importance of improving

‡‡ There are some applications where a short lifetime may be acceptable. For example, a solar cell used to power future low-cost, paper-based electronics may only have to last as long as the paper substrate itself. Even in such cases, however, the degradation process must be controllable—or at least predictable—to be useful.

the efficiency of large-area cells and integrated modules. Novel electrical and mechanical design strategies for integrating cells into efficient modules can also lead to lower cost.

PV module efficiency records can be up to 40% lower than small-area cell records, as shown in Fig. S12 in the ESI,† and typical commercial modules are less efficient still. Two primary types of losses occur in the transition from research lab to production line:

Intrinsic scaling losses. Scaling from small cells to large modules with multiple interconnected cells incurs physical scaling losses.

- Increase in cell size ($\sim$1 cm^2 to $\sim$100 cm^2): For technologies employing electrode grids (rather than transparent conducting electrodes alone), electrons must travel farther to reach an electrode in larger cells, resulting in higher resistive losses. Shadowing from electrodes reduces available light, while higher non-uniformity over large areas increases the likelihood of reverse current leakage (shunts).
- Increase in number of cells: Longer wires dissipate more power through resistive heating. Spacing between cells reduces the active area of the module. The output current of series-connected cells is limited by the lowest-performing cell.

Extrinsic manufacturing losses. While researchers often target the highest possible efficiencies without regard to cost, manufacturers may sacrifice efficiency to reduce cost, improve yield, and increase throughput.

- Process: Fabrication techniques that produce high efficiencies in the lab may be ineffective or too costly for large-scale manufacturing. Increasing production scale also increases contamination risk.[124]
- Materials: Research labs work primarily with small-area devices and can afford to use scarce, expensive, or high-purity materials, such as gold electrodes and high-quality glass substrates. Higher-quality materials may have fewer defects, lower recombination losses, and lower parasitic absorption (*e.g.*, in encapsulation and electrode materials).

Materials usage [g m^{-2} or g per W$_p$]

Reducing materials use has the potential to simultaneously reduce cost and enable new applications. Thinner substrates and active layers make cells lighter and more flexible. Lightweight cells and modules could reduce transportation and installation costs, while increased flexibility may help prevent breakage during shipping, installation, and operation. High specific power and flexibility are particularly valuable for mobile and BIPV applications. Furthermore, for thin-film cells, reducing layer thickness directly increases manufacturing throughput and decreases manufacturing cost per watt.

In quantifying material use, a useful metric is material intensity, measured in g per W$_p$. Material use (and cost) per peak watt is directly proportional to layer thickness and inversely proportional to efficiency. Reducing the material intensity of rare or expensive elements is particularly critical for scalability, and we encourage further investigation into abundant substitutes for such elements. One prominent example is the ongoing industry effort to replace screen-printed silver electrodes in c-Si solar cells with electroplated copper.[22] Approaches for reducing material intensity include epitaxial growth and release of thin c-Si or GaAs layers, optical engineering to enhance light absorption, and development of thin, lightweight substrates.

A related R&D direction deserving further attention is the development of novel material extraction and production strategies. A method for extracting tellurium more efficiently and cost-effectively from copper ores could improve significantly the prospects of CdTe PV for large-scale deployment. Emerging thin-film technologies would benefit from improved synthetic approaches for producing organic materials and colloidal QDs with high yield and high throughput. Synthetic methods with a small number of steps are essential for scalable, low-cost production.[125] Ultimately, addressing materials-use limitations for PV from both the production side and the consumption side is recommended.

Contribution of absorber and electrode materials to system cost

Here we analyze the contribution of different materials to PV system cost. Throughout this analysis, material intensity, specific power, and other performance parameters are calculated using record-efficiency or representative device structures and absorber compositions, assuming current certified record lab-cell efficiencies and 100% materials utilization and manufacturing yield. These optimistic assumptions may underestimate the amount of material required, but they provide a simple and traceable point of comparison. In practice, material utilization and manufacturing yields depend strongly on technological maturity and the processing strategy employed. Actual materials utilization has been estimated to range from 15–70% for a-Si:H, 60–80% for CIGS, and 90–99% for CdTe.[126] All performance parameters are calculated for III-V MJs based on the standard triple-junction structure shown in Fig. 3, for a-Si:H based on an a-Si:H/nc-Si:H/nc-Si:H triple-junction, for perovskite cells based on the mixed-halide perovskite $CH_3NH_3PbI_2Cl$, for organic cells based on a tandem polymer device, and for DSSCs based on the common N719 dye. A concentration ratio of 500$\times$ is assumed for III-V MJs unless otherwise specified.

Fig. 7 displays the material intensity, elemental abundance, and raw material cost for key elements used in different PV technologies. Technologies that tend toward the lower left corner of each plot can achieve large-scale deployment with lower risk of raw material cost and availability limitations. Silicon is abundant but used with high intensity in c-Si PV. Some commercial thin-film technologies, including CdTe and CIGS, employ scarce elements in relatively large quantities, which may limit their scalability.

Fig. 8 shows the cost of common PV electrode materials as a function of power conversion efficiency. At efficiencies below $\sim$10%, a 100 nm-thick Au electrode alone contributes over \$1 per W$_p$ to the cell cost, more than the current market price per peak watt for an entire c-Si PV module (\$0.65 per W$_p$ (ref. 109)).

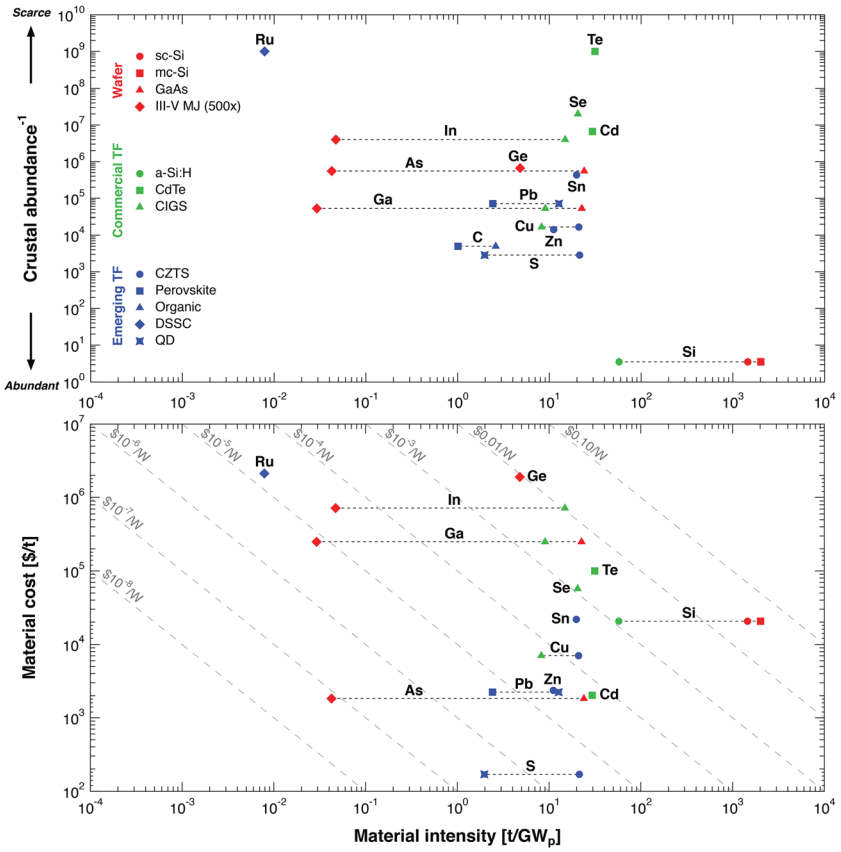

Fig. 7 Materials usage, abundance, and cost for key elements used in commercial and emerging PV technologies. Each element has an estimated crustal abundance[127] and thus a fixed position along the *y*-axis, but varies in position along the *x*-axis depending on technology-specific material needs. In the bottom plot, gray dashed lines indicate the contribution of raw material costs to the total cell cost in $ per W_p, assuming current market prices.

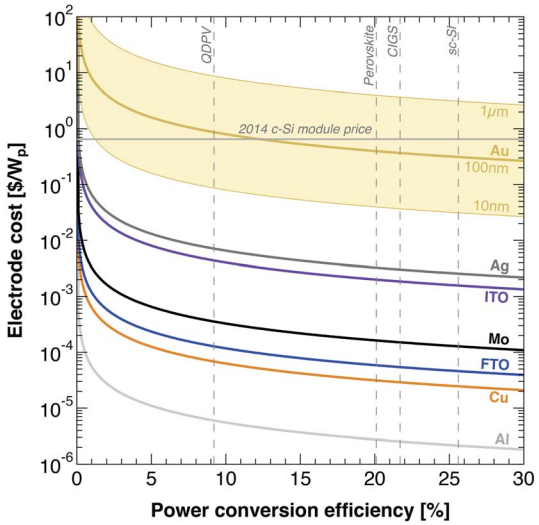

Fig. 8 Cost of common PV electrode materials as a function of power conversion efficiency. Raw material costs, based on current market prices, are shown for 100 nm-thick electrodes made of various metals and transparent conducting oxides. Curves for 10 nm and 1 μm are also shown for Au, commonly used in thin-film PV. Current record lab-cell efficiencies for several representative PV technologies are indicated by vertical dashed lines.

Manufacturing complexity and cost

The cost and footprint of manufacturing equipment for today's c-Si technologies may limit large-scale PV deployment. At current $1 per W_p investment costs for c-Si, a 1 GW_p per year factory requires a billion-dollar capital investment. Incremental reductions in manufacturing cost can be realized by making factories larger and improving supply-chain efficiency.[128] For thin films, moving from lab-scale batch processes to large-scale continuous processes will likely reduce manufacturing complexity and cost.[81] Lab-scale methods are often not feasible for high-volume manufacturing. For example, spin-coating of polymer and QD solutions wastes up to 90% of the starting material and is incompatible with high-throughput roll-to-roll processing. Increasing material deposition and manufacturing yield reduces costs and supports the materials-use targets discussed above.

No single PV technology today excels in all three of these technical characteristics: efficiency, materials use, and manufacturing cost. Today's emerging technologies are improving far faster than current deployed technologies improved in their early years, but it is important to note that the road to market and large-scale deployment is invariably long. Practical limits to PV deployment will depend on a wide range of technical, economic, and political factors, including the

material constraints discussed below. While we do not seek a "silver-bullet" technology—different applications may call for different solutions—it is clear that innovation opportunities exist for all PV technologies.

PV material scaling limits

Recent growth of the solar PV market has been rapid and unrelenting. Between 2000 and 2014, global grid-connected PV capacity grew from 1.3 GW_p to 139 GW_p,[129] a staggering 10 600% total increase at a compound annual growth rate of 43%—a doubling every two years. Despite this swift expansion, however, solar PV accounted for only 0.87% of global electricity production in 2013.[130] Combined with the contribution of other low-carbon technologies, this fraction must increase by up to two orders of magnitude by mid-century if dangerous anthropogenic interference with the Earth's climate is to be averted.[131,132] Such an ambitious target for deployment of solar power requires consideration of scaling of materials, manufacturing capacity, and land use.[13] This section principally focuses on materials constraints for terawatt-scale deployment of solar PV. We view materials requirements in the context of current global production levels,[126,133–136] using the metric of years of current production required to meet a deployment target. While we do not consider possible growth trajectories, others have extended this analysis by quantifying the rate at which materials production must grow to achieve particular deployment targets.[133–135]

Any quantitative analysis of PV scaling must make an assumption about future electricity demand and the fraction of that demand satisfied by PV (the solar fraction). The product of demand and solar fraction is the required annual solar generation in Wh per year; dividing this value by an assumed capacity factor and 8760 hours per year gives the installed PV capacity required, in W_p. Given a technology-dependent material intensity, installed capacity translates directly to material requirements.

Here we estimate the amount of key materials needed to satisfy 5%, 50%, or 100% of global electricity demand in 2050 with solar PV generation. The year 2050 is chosen to match globally recognized climate change mitigation targets.[132,137,138] In its 2 °C global warming scenario, the International Energy Agency forecasts a global electricity demand of 33 000 TWh in 2050.[139] This baseline demand, along with an average capacity factor of 15%,§§[15,118,140] is assumed for all calculations. We make the simplifying assumption that the power system can fully utilize solar generation regardless of its temporal profile. The 5%, 50%, and 100% solar fraction scenarios then translate to installed PV capacities of 1.25, 12.5, and 25 TW_p, respectively. We note that this analysis can be rescaled easily to accommodate different capacity targets and PV technology mixes. Although material issues are the focus of our analysis, realizing the aforementioned 2 °C scenario in practice will require wide-reaching changes in global energy systems and public policy, from upgrades in transmission and distribution grid infrastructure to addition of grid-scale energy storage to streamlining of regulatory procedures.[13]

§§ Current annual-average PV capacity factors range from ~11% in Germany to ~20% in the U.S., primarily due to differences in insolation.[118] Global-average capacity factors will likely increase with time, as deployment is expanding fastest in countries with higher insolation than Germany.[140] With an average irradiance over land[15] of 183 W m^{-2} and a typical DC-to-AC derate factor of ~0.8, we expect the long-term global average capacity factor to approach ~15%.

Commodity materials scaling

Here we consider common materials that are used in PV modules and systems but are not intrinsically required for solar cell operation. These commodity materials could be characterized as non-cell balance-of-system materials, and they share a number of properties that distinguish them from PV-critical materials. We classify as commodity materials:

- Flat glass – substrates, module encapsulation
- Plastic – environmental protection
- Concrete – system support structures
- Steel – system support structures
- Aluminum – module frame, racking, supports
- Copper – wiring

These commodity materials are abundant and are extracted or produced as primary products. Key influences on their long-term global production are thus market conditions and production capacity rather than elemental abundance. These materials are used in a variety of non-PV applications and are transferable between different end uses with little change in form; for example, the concrete and copper wiring used in a PV array are no different from the concrete and copper wiring used in an office building.

Our analysis of commodity materials is based on a technologically conservative vision of a future dominated by today's commercial technologies, including c-Si, CdTe, and CIGS. Since these systems are already in use and BOS requirements are well known, detailed projections of materials use under different scaling scenarios can be made. These projections are valid as long as module form factors do not change substantially. Estimates based on c-Si PV may constitute an upper bound on commodity materials usage: new PV technologies are likely to be competitive for grid-connected applications only if they can achieve lower BOS requirements than silicon, perhaps by employing lightweight and flexible modules with thin absorber layers.

Fig. 9 shows the absolute amount of each commodity material that must be produced between now and 2050 to deploy enough PV capacity to satisfy 5%, 50%, and 100% of global electricity demand in 2050. Comparison of material requirements with current annual production indicates how much commodity markets must expand to accommodate global PV demand. For example, current PV modules employ flat glass as substrates and encapsulation layers. To satisfy 50% of 2050 electricity demand with PV, corresponding to 12.5 TW_p of installed capacity, we need 626 million metric tons of glass. At the current flat glass production rate of 61 million metric tons per year, roughly 10 years' worth of production would have to be allocated for PV modules between now and 2050.

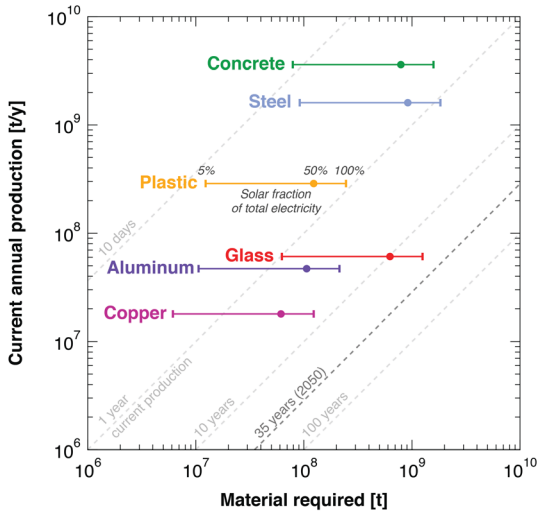

Fig. 9 Commodity material requirements for large-scale deployment of current PV technologies (primarily c-Si). For each commodity, we show the total amount of material required to deploy sufficient solar PV capacity to satisfy 5%, 50%, or 100% of global electricity demand in 2050. Gray dashed lines indicate the required increases in total production as a fraction or multiple of current annual production. Only flat glass, and to a lesser extent, copper and aluminum would require a significant expansion or redirection of production in order to achieve the material target under the 100% solar scenario. Material intensities are derived from DOE estimates.[135]

There appear to be no major commodity material constraints for terawatt-scale PV deployment through 2050, with the possible exception of flat glass at 100% solar electricity. For some commodities—glass, aluminum, and copper—the required production for a solar fraction of 100% (25 TW_p of peak capacity) exceeds 6 years at current annual production levels, which suggests that PV may eventually become a major driver for some commodity markets. However, we emphasize that future commodity material demand for other applications is not easily predictable. Current demand from PV constitutes a small fraction of total demand for each commodity considered in our analysis. More stringent constraints may arise for the critical elements used within each PV cell. These constraints are considered below.

Critical materials scaling

Today's PV technologies use chemical elements that differ greatly in abundance and annual production. Large-scale deployment of PV technologies that employ scarce elements would vastly increase demand for those elements. Unlike many other aspects of power systems, the use of scarce elements does not benefit from economies of scale. On the contrary, because they are genuinely scarce, the contribution of these elements to cell and module cost will likely increase with the scale of deployment in ways that are difficult to predict or control.

Here we consider possible constraints on solar PV deployment presented by PV-critical elements, defined as elements that are necessary components of certain PV technologies. Unlike commodity materials, these critical materials have few, if any, substitutes in a given PV technology. In most cases, they are part of the light-absorbing and charge-transporting layer; substituting another element would be akin to introducing a new and unproven technology. Critical materials availability constraints have been discussed in significant detail in the literature, particularly for commercial thin-film technologies.[126,136,141,142] In this work, we provide a unified analysis that includes all leading commercial and emerging PV technologies.

The absolute amount of any critical element is not expected to be a major constraint. Even supplying 100% of global electricity demand in 2050 with CdTe PV would only require on the order of 1/10 000 000 of the tellurium in the Earth's crust. However, the mining of any element¶¶ is only economical when it is concentrated far above its average crustal abundance. Most scarce elements are rarely found in concentrations high enough to warrant extraction as a primary product at today's prices: only a few rare elements, including gold, the platinum group elements, and sometimes silver, are so highly valued that they are mined as primary products. With the exception of silver and silicon, all of the critical elements used in deployed PV systems today are obtained as byproducts of the mining and refining of more abundant metals. For example, tellurium is found in copper, zinc, and lead ores, and is primarily obtained as a byproduct of the electrolytic refinement of copper.

Producing an element as a byproduct or co-product is typically much less expensive than producing the same element as a primary product because of economies of scope. The costs of investment capital, mine planning, permitting, extraction, haulage, and various refining steps are borne by the primary product.[13,143] As a result, the price and availability of critical byproducts depend strongly on the demand for the primary product. In addition, byproduction output is often sensitive to changes in the technology used to extract the primary product, making the demand-price function volatile and difficult to predict. Byproduction dynamics may restrict the annual production of critical elements until prices increase enough to warrant primary production, and it is likely that the resulting higher material costs will impede cost-effective PV deployment.

A detailed analysis of the economically recoverable fraction of these critical elements as a function of PV demand is beyond the scope of this study, but a comparison of the relative abundances of these elements provides a useful sense of scale when considering them as candidates for large-scale deployment. Silicon is 20 000 times as abundant as gallium and 300 000 000 times as abundant as tellurium. To supply 100% of global electricity in 2050 with c-Si PV would require roughly one-third as much silicon and one-half as much silver as has been produced since 1900. Complete reliance on CdTe or CIGS PV, on the other hand, would require over 75 times more tellurium or gallium for PV than has ever been produced for all other uses combined.

While necessary, raw elemental availability is not a sufficient condition for ramping up to TW-scale PV production. The scalability of annual global production of PV-critical elements at

¶¶ Apart perhaps from the eight major rock-forming elements (O, Si, Al, Fe, Ca, Na, K, and Mg), which are all present at crustal abundances above 2%.

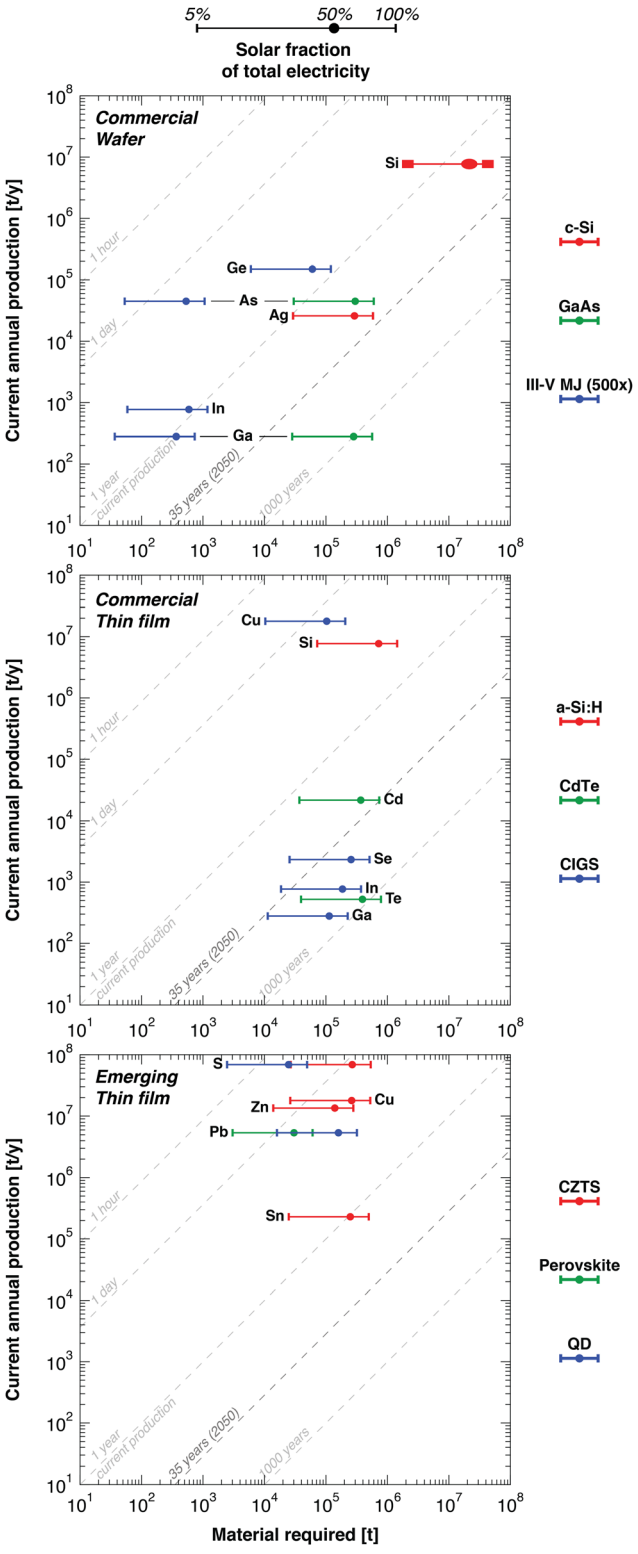

Fig. 10 Critical material requirements for large-scale deployment of wafer-based, commercial thin-film, and emerging thin-film solar cell technologies. For each PV technology, we show the amount of key elements required to satisfy 5%, 50%, or 100% of global electricity demand in 2050, corresponding to a total installed capacity of ~1.25 TW_p, 12.5 TW_p, or 25 TW_p. Gray dashed lines indicate material requirements as a multiple of current annual production. Technologies that tend toward the upper-left corner of each plot can achieve terawatt-scale deployment without substantial growth in annual production of constituent elements. Boxes and oval for c-Si represent the range spanned by sc-Si and mc-Si technologies. Organic and dye-sensitized solar cells require only abundant elements and are omitted.

required purities may be more relevant than crustal abundance. Production and price are not necessarily linked to abundance: while silver is one of the least abundant elements considered here, it has been highly valued for millennia, and primary mining of silver is a well-established industry. Selenium costs less and is more copiously produced than gallium and indium, even though it is the least abundant of the three. Furthermore, as pointed out by Kavlak *et al.*,[133,134] limits to the rate of growth in the production of particular elements may hinder aggressive growth in the deployment of particular PV technologies.

In Fig. 10, which mirrors the format of Fig. 9, we compare the total amount of key elements required to satisfy 5%, 50%, and 100% of global electricity demand in 2050 with today's wafer-based, commercial thin-film, and emerging thin-film PV technologies. Total material requirements are plotted against current annual production[144,145] to provide a sense of scale.

To supply 100% of 2050 global electricity demand with CdTe PV, we need similar amounts of cadmium and tellurium: 737 000 metric tons and 786 000 metric tons, respectively. Both elements thus appear at roughly the same position along the horizontal axis. But current annual cadmium production (21 800 t per year) exceeds tellurium production (525 t per year) by two orders of magnitude. As a result, tellurium lies far below cadmium on the vertical axis. Deploying 25 TW_p of CdTe PV would require the equivalent of 34 years of global cadmium production and 1500 years of global tellurium production at current rates.

We find that c-Si PV could meet 100% of electricity demand by 2050 without major material constraints, assuming the use of silver contacts can be reduced or eliminated. The same cannot be said for technologies based on tellurium, indium, and other scarce elements. This is consistent with the findings of previous studies.[126,133,134] Current commercial thin-film technologies would need to demonstrate dramatic reductions in active material intensity to fulfill a large fraction of electricity demand. Approaches to mitigating potential critical material scaling limits include (1) decreasing the material intensity of presently-used elements and (2) developing thin-film technologies that employ more abundant and widely produced elements.

For some commercial PV technologies, the required reductions in material intensity may be prohibitively large, given physical and practical limits on layer thicknesses. For example, thinner films may be unable to absorb sunlight fully or may aggravate shorting in large-area cells. Avoiding scarce elements altogether is thus desirable. Many emerging technologies require less material than commercial technologies and use only Earth-abundant elements.

Returning to Fig. 10, a stark contrast arises between material requirements for commercial and emerging thin-film PV technologies. Consider colloidal quantum dot PV: deploying 25 TW_p

of PbS QDPV would require the equivalent of only 22 days of global lead production and 6 hours of global sulfur production. This disparity can be attributed to the use of abundant, high-production-volume primary metals and ultra-thin absorber layers.

Materials scaling considerations may be a deciding factor in determining which technologies fulfill the majority of PV demand in the coming decades. We emphasize however that no single PV technology is likely to capture 100% of the PV market. Commercial thin-film technologies could avoid critical material constraints and remain viable at a deployment scale of up to hundreds of gigawatts by 2050. Furthermore, emerging thin films have not reached the scale needed to precisely quantify materials utilization and manufacturing yield in high-volume module production, although the order-of-magnitude conclusions discussed above should remain valid in the absence of disruptive technological change.

Conclusion

Predicting the future development of any technology is by nature fraught with uncertainty. While crystalline silicon dominates the PV market today, alternative technologies are evolving rapidly. The solar cell of the future may be a refined version of current commercial cells or an entirely new technology. Furthermore, global installed PV capacity today is a miniscule fraction of expected future deployment. Few—if any—industries have grown as fast or as unpredictably as the PV industry in recent years.

Faced with uncertain technological change and uncertain economic pressures, we abstain from betting on any particular PV technology. Instead, we view all technologies through the objective lens of application-driven performance metrics. These metrics guide us toward three technical themes—increased efficiencies, reduced materials usage, and reduced manufacturing complexity and cost—that technology leaders should target in their R&D efforts. By focusing on the unique strengths and potential applications of solar photovoltaics, we can identify windows of opportunity for future PV technology development and deployment.

Acknowledgements

This work emerged from the authors' involvement in the MIT Future of Solar Energy Study. We thank Andrea Maurano, Frank O'Sullivan, Dick Schmalensee, Bob Armstrong, Rob Stoner, John Deutch, Henry Jacoby, John Parsons, Gary DesGroseilliers, Doug Powell, and the entire Solar Study team for constructive guidance. We thank Riley Brandt for valuable discussions and suggestions on the graphical representation of data. We thank Sam Stranks for input on perovskite and DSSC technologies, Gökşin Kavlak and Jessika Trancik for discussions on materials scaling, Becca Jones-Albertus for valuable insight on III-V multijunctions, Lidija Šekarić for policy and market perspectives, and Nathan Lewis for his comments on initial drafts of this work.

Notes and references

1 A. Luque, A. Martí and A. J. Nozik, *MRS Bull.*, 2007, **32**, 236–241.
2 D. Ginley, M. A. Green and R. Collins, *MRS Bull.*, 2008, **33**, 355–364.
3 A. E. Curtright, M. G. Morgan and D. W. Keith, *Environ. Sci. Technol.*, 2008, **42**, 9031–9038.
4 L. L. Kazmerski, *J. Electron Spectrosc. Relat. Phenom.*, 2006, **150**, 105–135.
5 L. L. Kazmerski, *Renewable Sustainable Energy Rev.*, 1997, **1**, 71–170.
6 M. A. Green, *Prog. Photovoltaics*, 2001, **9**, 123–135.
7 M. A. Green, *Phys. E*, 2002, **14**, 65–70.
8 M. A. Green, *Sol. Energy*, 2003, **74**, 181–192.
9 M. A. Green, *J. Mater. Sci.: Mater. Electron.*, 2007, **18**, S15–S19.
10 G. Conibeer, *Mater. Today*, 2007, **10**, 42–50.
11 C. Fröhlich and J. Lean, *Astron. Astrophys. Rev.*, 2004, **12**, 273–320.
12 Solar System Exploration, National Aeronautics and Space Administration, http://solarsystem.nasa.gov/planets, accessed 18 September 2014.
13 MIT Future of Solar Energy Study, in press.
14 Solar Data: Lower 48 and Hawaii GHI 10km Resolution 1998 to 2009, National Renewable Energy Laboratory, 2012, http://www.nrel.gov/gis/data_solar.html, accessed 18 September 2014.
15 M. Z. Jacobson and M. A. Delucchi, *Energy Policy*, 2011, **39**, 1154–1169.
16 NREL Solar Radiation Research Laboratory: Baseline Measurement System (BMS), http://www.nrel.gov/midc/srrl_bms/, accessed 18 September 2014.
17 E. K. Hart, E. D. Stoutenburg and M. Z. Jacobson, *Proc. IEEE*, 2012, **100**, 322–334.
18 Solar Resources By Class Per Country, National Renewable Energy Laboratory, http://en.openei.org/datasets/dataset/solar-resources-by-class-and-country, accessed 2 February 2015.
19 World DataBank: World Development Indicators, The World Bank, http://databank.worldbank.org, accessed 18 September 2014.
20 Maps of Irradiation, Irradiance, and UV, Solar Radiation Data (SoDa), http://www.soda-is.com, accessed 2 February 2015.
21 B. Rankin, Radical Cartography, 2008, http://www.radicalcartography.net, accessed 18 September 2014.
22 2013 Results, International Technology Roadmap for Photovoltaic (ITRPV), 2014.
23 J. Czochralski, *Z. Phys. Chem.*, 1918, **92**, 219.
24 G. K. Teal and J. B. Little, *Phys. Rev.*, 1950, **78**, 647.
25 T. Kinoshita, D. Fujishima, A. Yano, A. Ogane, S. Tohoda, K. Matsuyama, Y. Nakamura, N. Tokuoka, H. Kanno, H. Sakata, M. Taguchi and E. Maruyama, *Proceedings of the 26th European Photovoltaic Solar Energy Conference and Exhibition*, Hamburg, 2011, pp. 871–874.

26 Y. Tsunomura, Y. Yoshimine, M. Taguchi, T. Baba, T. Kinoshita, H. Kanno, H. Sakata, E. Maruyama and M. Tanaka, *Sol. Energy Mater. Sol. Cells*, 2009, **93**, 670–673.
27 Best Research-Cell Efficiencies (rev. 12-18-2014), National Renewable Energy Laboratory, 2014.
28 M. A. Green, K. Emery, Y. Hishikawa, W. Warta and E. D. Dunlop, *Prog. Photovoltaics*, 2015, **23**, 1–9.
29 S. Wang, B. D. Weil, Y. Li, K. X. Wang, E. Garnett, S. Fan and Y. Cui, *Nano Lett.*, 2013, **13**, 4393–4398.
30 A. Wang, J. Zhao, S. R. Wenham and M. A. Green, *Prog. Photovoltaics*, 1996, **4**, 55–58.
31 *Handbook of Photovoltaic Science and Engineering*, ed. A. Luque and S. Hegedus, 2nd edn, 2011.
32 I. Gordon, F. Dross, V. Depauw, A. Masolin, Y. Qiu, J. Vaes, D. Van Gestel and J. Poortmans, *Sol. Energy Mater. Sol. Cells*, 2011, **95**, S2–S7.
33 J. H. Petermann, D. Zielke, J. Schmidt, F. Haase, E. G. Rojas and R. Brendel, *Prog. Photovoltaics*, 2011, **20**, 1–5.
34 E. Kobayashi, N. Kusunoki, Y. Watabe, R. Hao and T. S. Ravi, *6th World Conference on Photovoltaic Energy Conversion (WCPEC-6) Technical Digest*, Kyoto, 2014.
35 S. Varlamov, J. Dore, R. Evans, D. Ong, B. Eggleston, O. Kunz, U. Schubert, T. Young, J. Huang, T. Soderstrom, K. Omaki, K. Kim, A. Teal, M. Jung, J. Yun, Z. M. Pakhuruddin, R. Egan and M. A. Green, *Sol. Energy Mater. Sol. Cells*, 2013, **119**, 246–255.
36 M. A. Green, *Appl. Phys. A*, 2009, **96**, 153–159.
37 M. A. Green, *Sol. Energy*, 2004, **77**, 857–863.
38 E. Yablonovitch, T. Gmitter, J. P. Harbison and R. Bhat, *Appl. Phys. Lett.*, 1987, **51**, 2222–2224.
39 R. Jones-Albertus, E. Becker, R. Bergner, T. Bilir, D. Derkacs, O. Fidaner, D. Jory, T. Liu, E. Lucow, P. Misra, E. Pickett, F. Suarez, A. Sukiasyan, T. Sun, L. Zhang, V. Sabnis, M. Wiemer and H. Yuen, *MRS Proc.*, 2013, **1538**, 161–166.
40 R. R. King, D. C. Law, K. M. Edmondson, C. M. Fetzer, G. S. Kinsey, H. Yoon, R. A. Sherif and N. H. Karam, *Appl. Phys. Lett.*, 2007, **90**, 183516.
41 P. T. Chiu, D. C. Law, R. L. Woo, S. B. Singer, D. Bhusari, W. D. Hong, A. Zakaria, J. Boisvert, S. Mesropian, R. R. King and N. H. Karam, *IEEE J. Photovolt.*, 2014, **4**, 493–497.
42 R. R. King, D. Bhusari, D. Larrabee, X.-Q. Liu, E. Rehder, K. Edmondson, H. Cotal, R. K. Jones, J. H. Ermer, C. M. Fetzer, D. C. Law and N. H. Karam, *Prog. Photovoltaics*, 2012, **20**, 801–815.
43 A. V. Shah, H. Schade, M. Vanecek, J. Meier, E. Vallat-Sauvain, N. Wyrsch, U. Kroll, C. Droz and J. Bailat, *Prog. Photovoltaics*, 2004, **12**, 113–142.
44 Photovoltaics Report, Fraunhofer ISE, 2014.
45 D. L. Staebler and C. R. Wronski, *Appl. Phys. Lett.*, 1977, **31**, 292–294.
46 V. Fthenakis and K. Zweibel, *CdTe PV: Real and Perceived EHS Risks*, National Center for Photovoltaics Review Meeting, Denver, 2003.
47 F. Kessler and D. Rudmann, *Sol. Energy*, 2004, **77**, 685–695.
48 M. J. Hetzer, Y. M. Strzhemechny, M. Gao, M. A. Contreras, A. Zunger and L. J. Brillson, *Appl. Phys. Lett.*, 2005, **86**, 162105.
49 J. Werner, J. Mattheis and U. Rau, *Thin Solid Films*, 2005, **480–481**, 399–409.
50 S. Nishiwaki, S. Siebentritt, P. Walk and M. Ch. Lux-Steiner, *Prog. Photovoltaics*, 2003, **11**, 243–248.
51 D. D. Hsu, P. O'Donoughue, V. Fthenakis, G. A. Heath, H. C. Kim, P. Sawyer, J.-K. Choi and D. E. Turney, *J. Ind. Ecol.*, 2012, **16**, S122–S135.
52 H. C. Kim, V. Fthenakis, J.-K. Choi and D. E. Turney, *J. Ind. Ecol.*, 2012, **16**, S110–S121.
53 T. K. Todorov, J. Tang, S. Bag, O. Gunawan, T. Gokmen, Y. Zhu and D. B. Mitzi, *Adv. Energy Mater.*, 2013, **3**, 34–38.
54 H. Katagiri, K. Jimbo, W. S. Maw, K. Oishi, M. Yamazaki, H. Araki and A. Takeuchi, *Thin Solid Films*, 2009, **517**, 2455–2460.
55 B. G. Mendis, M. D. Shannon, M. C. Goodman, J. D. Major, R. Claridge, D. P. Halliday and K. Durose, *Prog. Photovoltaics*, 2014, **22**, 24–34.
56 W. Wang, M. T. Winkler, O. Gunawan, T. Gokmen, T. K. Todorov, Y. Zhu and D. B. Mitzi, *Adv. Energy Mater.*, 2013, **4**, 1301465.
57 H.-S. Kim, C.-R. Lee, J.-H. Im, K.-B. Lee, T. Moehl, A. Marchioro, S.-J. Moon, R. Humphry-Baker, J.-H. Yum, J. E. Moser, M. Grätzel and N.-G. Park, *Sci. Rep.*, 2012, **2**, 591–597.
58 M. M. Lee, J. Teuscher, T. Miyasaka, T. N. Murakami and H. J. Snaith, *Science*, 2012, **338**, 643–647.
59 M. A. Green, A. Ho-Baillie and H. J. Snaith, *Nat. Photonics*, 2014, **8**, 506–514.
60 H. J. Snaith, *J. Phys. Chem. Lett.*, 2013, **4**, 3623–3630.
61 S. D. Stranks and H. J. Snaith, submitted.
62 G. E. Eperon, S. D. Stranks, C. Menelaou, M. B. Johnston, L. M. Herz and H. J. Snaith, *Energy Environ. Sci.*, 2014, **7**, 982–988.
63 N. K. Noel, S. D. Stranks, A. Abate, C. Wehrenfennig, S. Guarnera, A.-A. Haghighirad, A. Sadhanala, G. E. Eperon, S. K. Pathak, M. B. Johnston, A. Petrozza, L. M. Herz and H. J. Snaith, *Energy Environ. Sci.*, 2014, **7**, 3061–3068.
64 F. Hao, C. C. Stoumpos, D. H. Cao, R. P. H. Chang and M. G. Kanatzidis, *Nat. Photonics*, 2014, **8**, 489–494.
65 J. H. Noh, S. H. Im, J. H. Heo, T. N. Mandal and S. I. Seok, *Nano Lett.*, 2013, **13**, 1764–1769.
66 J. Burschka, N. Pellet, S.-J. Moon, R. Humphry-Baker, P. Gao, M. K. Nazeeruddin and M. Grätzel, *Nature*, 2013, **499**, 316–319.
67 M. Liu, M. B. Johnston and H. J. Snaith, *Nature*, 2013, **501**, 395–398.
68 S. D. Stranks, P. K. Nayak, W. Zhang, T. Stergiopoulos and H. J. Snaith, *Angew. Chem., Int. Ed.*, 2015, DOI: 10.1002/anie.201410214.
69 S. D. Stranks, G. E. Eperon, G. Grancini, C. Menelaou, M. J. P. Alcocer, T. Leijtens, L. M. Herz, A. Petrozza and H. J. Snaith, *Science*, 2013, **342**, 341–344.

70 G. Xing, N. Mathews, S. Sun, S. S. Lim, Y. M. Lam, M. Grätzel, S. Mhaisalkar and T. C. Sum, *Science*, 2013, **342**, 344–347.
71 J. M. Ball, M. M. Lee, A. Hey and H. J. Snaith, *Energy Environ. Sci.*, 2013, **6**, 1739–1743.
72 P. Peumans, A. Yakimov and S. R. Forrest, *J. Appl. Phys.*, 2003, **93**, 3693.
73 M. Riede, T. Mueller, W. Tress, R. Schueppel and K. Leo, *Nanotechnology*, 2008, **19**, 424001.
74 S. Günes, H. Neugebauer and N. S. Sariciftci, *Chem. Rev.*, 2007, **107**, 1324–1338.
75 K. M. Coakley and M. D. McGehee, *Chem. Mater.*, 2004, **16**, 4533–4542.
76 G. Li, R. Zhu and Y. Yang, *Nat. Photonics*, 2012, **6**, 153–161.
77 S. E. Shaheen, D. S. Ginley and G. E. Jabbour, *MRS Bull.*, 2005, **30**, 10–19.
78 B. Kippelen and J.-L. Brédas, *Energy Environ. Sci.*, 2009, **2**, 251–261.
79 H. Hoppe and N. S. Sariciftci, *J. Mater. Res.*, 2004, **19**, 1924–1945.
80 D. Wöhrle and D. Meissner, *Adv. Mater.*, 1991, **3**, 129–138.
81 F. C. Krebs, *Sol. Energy Mater. Sol. Cells*, 2009, **93**, 394–412.
82 J. Y. Kim, K. Lee, N. E. Coates, D. Moses, T.-Q. Nguyen, M. Dante and A. J. Heeger, *Science*, 2007, **317**, 222–225.
83 K. Kawano, R. Pacios, D. Poplavskyy, J. Nelson, D. D. C. Bradley and J. R. Durrant, *Sol. Energy Mater. Sol. Cells*, 2006, **90**, 3520–3530.
84 R. R. Lunt, T. P. Osedach, P. R. Brown, J. A. Rowehl and V. Bulović, *Adv. Mater.*, 2011, **23**, 5712–5727.
85 A. Hagfeldt, G. Boschloo, L. Sun, L. Kloo and H. Pettersson, *Chem. Rev.*, 2010, **110**, 6595–6663.
86 M. Grätzel, *Inorg. Chem.*, 2005, **44**, 6841–6851.
87 M. Grätzel, *J. Photochem. Photobiol., C*, 2003, **4**, 145–153.
88 M. K. Nazeeruddin, P. Péchy, T. Renouard, S. M. Zakeerudin, R. Humphry-Baker, P. Comte, P. Liska, L. Cevey, E. Costa, V. Shklover, L. Spiccia, G. B. Deacon, C. A. Bignozzi and M. Grätzel, *J. Am. Chem. Soc.*, 2001, **123**, 1613–1624.
89 H. J. Snaith and L. Schmidt-Mende, *Adv. Mater.*, 2007, **19**, 3187–3200.
90 I. Chung, B. Lee, J. He, R. P. H. Chang and M. G. Kanatzidis, *Nature*, 2012, **485**, 486–489.
91 U. Bach, D. Lupo, P. Comte, J. E. Moser, F. Weissörtel, J. Salbech, H. Spreitzer and M. Grätzel, *Nature*, 1998, **395**, 583–585.
92 A. Yella, H.-W. Lee, H. N. Tsao, C. Yi, A. K. Chandiran, M. K. Nazeeruddin, E. W.-G. Diau, C.-Y. Yeh, S. M. Zakeeruddin and M. Grätzel, *Science*, 2011, **334**, 629–634.
93 X. Lan, S. Masala and E. H. Sargent, *Nat. Mater.*, 2014, **13**, 233–240.
94 O. E. Semonin, J. M. Luther and M. C. Beard, *Mater. Today*, 2012, **15**, 508–515.
95 J. Tang and E. H. Sargent, *Adv. Mater.*, 2011, **23**, 12–29.
96 E. H. Sargent, *Nat. Photonics*, 2009, **3**, 325–331.
97 P. V. Kamat, *J. Phys. Chem. C*, 2008, **112**, 18737–18753.
98 E. H. Sargent, *Adv. Mater.*, 2005, **17**, 515–522.
99 J. J. Choi, W. N. Wenger, R. S. Hoffman, Y.-F. Lim, J. Luria, J. Jasieniak, J. A. Marohn and T. Hanrath, *Adv. Mater.*, 2011, **23**, 3144–3148.
100 X. Wang, G. I. Koleilat, J. Tang, H. Liu, I. J. Kramer, R. Debnath, L. Brzozowski, D. A. R. Barkhouse, L. Levina, S. Hoogland and E. H. Sargent, *Nat. Photonics*, 2011, **5**, 480–484.
101 C. M. Chuang, P. R. Brown, V. Bulović and M. G. Bawendi, *Nat. Mater.*, 2014, **13**, 796–801.
102 P. R. Brown, D. Kim, R. R. Lunt, N. Zhao, M. G. Bawendi, J. C. Grossman and V. Bulović, *ACS Nano*, 2014, **8**, 5863–5872.
103 A. H. Ip, S. M. Thon, S. Hoogland, O. Voznyy, D. Zhitomirsky, R. Debnath, L. Levina, L. R. Rollny, G. H. Carey, A. Fischer, K. W. Kemp, I. J. Kramer, Z. Ning, A. J. Labelle, K. W. Chou, A. Amassian and E. H. Sargent, *Nat. Nanotechnol.*, 2012, **7**, 577–582.
104 J. Jasieniak, M. Califano and S. E. Watkins, *ACS Nano*, 2011, **5**, 5888–5902.
105 J. Tang, K. W. Kemp, S. Hoogland, K. S. Jeong, H. Liu, L. Levina, M. Furukawa, X. Wang, R. Debnath, D. Cha, K. W. Chou, A. Fischer, A. Amassian, J. B. Asbury and E. H. Sargent, *Nat. Mater.*, 2011, **10**, 765–771.
106 D. D. Wanger, R. E. Correa, E. A. Dauler and M. G. Bawendi, *Nano Lett.*, 2013, **13**, 5907–5912.
107 D. Zhitomirsky, O. Voznyy, L. Levina, S. Hoogland, K. W. Kemp, A. H. Ip, S. M. Thon and E. H. Sargent, *Nat. Commun.*, 2014, **5**, 3803.
108 Average Commercial Module Efficiency, First Solar *vs.* Crystalline Silicon, 2009-2017E, GTM Research PV Pulse, 2014, http://www.greentechmedia.com/articles/read/could-first-solars-thin-film-beat-silicon-pv-on-efficiency, accessed 18 September 2014.
109 Module Price Index, pvXchange, 2015, http://www.pvxchange.com, accessed 3 February 2015.
110 W. A. MacDonald, M. K. Looney, D. MacKerron, R. Eveson, R. Adam, K. Hashimoto and K. Rakos, *J. Soc. Inf. Disp.*, 2007, **15**, 1075–1083.
111 J. You, Z. Hong, Y. Yang, Q. Chen, M. Cai, T.-B. Song, C.-C. Chen, S. Lu, Y. Liu, H. Zhou and Y. Yang, *ACS Nano*, 2014, **8**, 1674–1680.
112 M. C. Barr, J. A. Rowehl, R. R. Lunt, J. Xu, A. Wang, C. M. Boyce, S. G. Im, V. Bulović and K. K. Gleason, *Adv. Mater.*, 2011, **23**, 3500–3505.
113 R. R. Lunt and V. Bulović, *Appl. Phys. Lett.*, 2011, **98**, 113305.
114 R. Betancur, P. Romero-Gomez, A. Martinez-Otero, X. Elias, M. Maymó and J. Martorell, *Nat. Photonics*, 2013, **7**, 995–1000.
115 R. Schmalensee, The Performance of U.S. Wind and Solar Generating Plants, MIT Center for Energy and Environmental Policy Research, 2013.
116 G. Barbose, N. Darghouth, S. Weaver and R. Wiser, *Tracking the Sun VI: An Historical Summary of the Installed Price of Photovoltaics in the United States from 1998 to 2012*, 2013, Lawrence Berkeley National Laboratory, 2013.
117 M. A. Green, *Proc. SPIE*, 2014, **8981**, 89810L.

118 Electric Power Monthly with Data for December 2013, U.S. Energy Information Administration, 2014, http://www.eia.gov/electricity/monthly/current_year/february2014.pdf, accessed 18 September 2014.
119 E. Fortunato, D. Ginley, H. Hosono and D. C. Paine, *MRS Bull.*, 2007, **32**, 242–247.
120 D. S. Hecht and R. B. Kaner, *MRS Bull.*, 2011, **36**, 749–755.
121 W. Shockley and H. J. Queisser, *J. Appl. Phys.*, 1961, **32**, 510–519.
122 C. H. Henry, *J. Appl. Phys.*, 1980, **51**, 4494.
123 M. C. Hanna and A. J. Nozik, *J. Appl. Phys.*, 2006, **100**, 074510.
124 B. Rech, C. Beneking and S. Wieder, *Proceedings of the 2nd World Conference and Exhibition on Photovoltaic Solar Energy Conversion*, Vienna, 1998, pp. 391–396.
125 T. P. Osedach, T. L. Andrew and V. Bulović, *Energy Environ. Sci.*, 2013, **6**, 711–718.
126 B. A. Andersson, *Prog. Photovoltaics*, 2000, **8**, 61–76.
127 CRC Handbook of Chemistry and Physics, 95th Edition, 2014–15, Taylor and Francis, 2014, www.hbcpnetbase.com, accessed 18 September 2014.
128 A. C. Goodrich, D. M. Powell, T. L. James, M. Woodhouse and T. Buonassisi, *Energy Environ. Sci.*, 2013, **6**, 2811–2821.
129 Global Market Outlook for Photovoltaics 2014–2018, European Photovoltaic Industry Association, 2014.
130 Trends in Photovoltaic Applications, 19th Edition, International Energy Agency Photovoltaic Power Systems Programme, 2014.
131 United Nations Framework Convention on Climate Change, United Nations, 1992.
132 M. I. Hoffert, K. Caldeira, A. K. Jain, E. F. Haites, L. D. D. Harvey, S. D. Potter, M. E. Schlesinger, S. H. Schneider, R. G. Watts, T. M. L. Wigley and D. J. Wuebbles, *Nature*, 1998, **395**, 881–884.
133 G. Kavlak, J. McNerney, R. L. Jaffe and J. E. Trancik, *IEEE Photovoltaic Spec. Conf., 40th*, Denver, 2014, pp. 1442–1447.
134 G. Kavlak, J. McNerney, R. L. Jaffe and J. E. Trancik, 2014, arXiv:1501.03039.
135 PV FAQs: Does the World Have Enough Materials for PV to Help Address Climate Change?, U.S. Department of Energy, 2005.
136 C. Wadia, A. P. Alivisatos and D. M. Kammen, *Environ. Sci. Technol.*, 2009, **43**, 2072–2077.
137 Intergovernmental Panel on Climate Change 5th Assessment Report, Climate Change 2014: Mitigation of Climate Change, 2014.
138 M. Meinshausen, N. Meinshausen, W. Hare, S. C. B. Raper, K. Frieler, R. Knutti, D. J. Frame and M. R. Allen, *Nature*, 2009, **458**, 1158–1163.
139 Energy Technology Perspectives 2014, International Energy Agency, 2014.
140 H. Wirth, *Recent Facts about Photovoltaics in Germany*, Fraunhofer ISE, 2014.
141 V. Fthenakis, *Renewable Sustainable Energy Rev.*, 2009, **13**, 2746–2750.
142 M. Woodhouse, A. Goodrich, R. Margolis, T. James, R. Dhere, T. Gessert, T. Barnes, R. Eggert and D. Albin, *Sol. Energy Mater. Sol. Cells*, 2013, **115**, 199–212.
143 R. Jaffe, J. Price, G. Ceder, R. Eggert, T. Graedel, K. Gschneidner, M. Hitzman, F. Houle, A. Hurd, R. Kelley, A. King, D. Milliron, B. Skinner and F. Slakey, *Energy Critical Elements: Securing Materials for Emerging Technologies*, American Physical Society/Materials Research Society, 2011.
144 *Minerals Yearbook: Volume I – Metals and Minerals*, U.S. Geological Survey, 2011.
145 *Mineral Commodity Summaries 2014*, U.S. Geological Survey, 2014.

Electronic Supplementary Information (ESI) *for* Pathways for Solar Photovoltaics

Joel Jean[a], Patrick R. Brown[b], Robert L. Jaffe[b,c], Tonio Buonassisi[d], and Vladimir Bulović[a]

[a]*Department of Electrical Engineering and Computer Science, Massachusetts Institute of Technology, 77 Massachusetts Ave., Cambridge, MA, 02139.*
[b]*Department of Physics, Massachusetts Institute of Technology*
[c]*Center for Theoretical Physics, Massachusetts Institute of Technology*
[d]*Department of Mechanical Engineering, Massachusetts Institute of Technology*

Glossary of Terms

Balance-of-system (BOS): All components of an installed solar PV system besides PV modules. This term typically includes both hardware (e.g., inverter, transformer, wiring, and racking) and non-hardware (e.g., installation labor, customer acquisition, permitting, inspection, interconnection, sales tax, and financing) costs.

Bandgap: Fundamental property of semiconducting materials that determines the minimum energy (maximum wavelength) of light that can be absorbed, in units of electron-volts (eV). Direct-bandgap materials (e.g., GaAs, CdTe, and PbS) absorb light much more efficiently than indirect-bandgap materials (e.g., Si and Ge), reducing the required absorber thickness.

Byproduction: Production of an element as a secondary product of the mining and refinement of a major (primary) metal. Byproduction can reduce raw material prices substantially due to economies of scope, but the associated price volatility and production ceiling make byproduced elements a potential obstacle to large-scale deployment of some PV technologies.

Capacity factor (CF): The ratio of the actual AC energy output [kWh/y] of a PV system to the output of an ideal system with the same nameplate capacity and no DC-to-AC conversion losses, under constant peak irradiance (1000 W/m^2) and at 25ºC. Capacity factors are often used to compare electric power generation systems.

Commodity materials: Abundant materials (e.g., glass, concrete, and steel) that are used in PV modules and systems as well as a variety of non-PV applications. The cost and availability of commodity materials are typically determined by market conditions and production capacity rather than raw abundance.

Critical materials: Elements used in the active absorber or electrode layers of PV cells. Critical materials are often mined as byproducts and typically have few available substitutes for a given PV technology without sacrificing performance.

Crustal abundance: The relative concentration of a chemical element in the Earth's upper continental crust (top ~15 km), typically reported in units of parts per million (ppm) by mass.[1] Oxygen and silicon are the two most abundant elements in the crust.

Energy yield: The actual energy output of a PV module or system divided by the nameplate DC capacity, in units of kWh/kW_p or hours. The energy yield of a PV module or system over a given time period corresponds to the number of hours for which it would need to operate at peak power

to produce the same amount of energy.

Exciton: An electron-hole pair bound together by electrostatic attraction. Excitons are neutral quasi-particles that are formed when light is absorbed in a semiconductor; they must be separated into free charges to contribute to photocurrent. Excitons in conventional inorganic semiconductors (Wannier-Mott excitons) are weakly bound and tend to dissociate shortly after formation. Excitons in many emerging thin-film PV materials such as organic small molecules and polymers (Frenkel excitons) are more strongly confined and only dissociate when they encounter a heterojunction interface (i.e., between two energetically dissimilar materials).

Form factor: General term that refers to the physical characteristics of a solar cell or module, including dimensions, weight, and flexibility.

Insolation: A measure of the solar energy received over a given area over a given time period, typically in units of kWh/m^2/day. "Insolation" is a contraction of the phrase "incoming solar radiation." When the time unit in the denominator is omitted, the period of observation must be specified (e.g., "an average daily insolation of 4.5 kWh/m^2"). The term "irradiation" is sometimes used interchangeably with "insolation."

Intermittency: Temporal variation in the availability of sunlight and hence PV panel output over varying time scales, from seconds to days to seasons. Intermittency can be caused by unpredictable (stochastic) cloud cover and weather or by predictable (deterministic) diurnal, seasonal, and climatic variations.

Irradiance: A measure of the solar energy received over a given area, typically in units of W/m^2. The average irradiance over a given time period is equal to the insolation over the same period.

Lattice mismatch: A situation that occurs when a crystalline semiconductor is deposited directly (epitaxially) on another crystalline material with a different lattice constant (physical dimension of repeating unit cells in a crystal). When the mismatch is large, defects (dislocations) are likely to arise, increasing recombination and decreasing PV performance. Lattice matching is a key consideration for III-V MJ solar cells, which consist of many stacked epitaxial films with different lattice constants. Lattice-mismatched approaches avoid the need for lattice matching by incorporating a "metamorphic" buffer layer with graded composition to accommodate mismatch.

Levelized cost of energy (LCOE): Also known as levelized cost of electricity; total cost per unit of electrical energy produced by an electric power system, in units of $/kWh or ¢/kWh. A complete calculation of levelized cost of energy includes the effect of actual system output (as measured by the performance ratio or capacity factor), upfront capital costs, fixed and variable operation and maintenance (O&M) costs (including fuel where applicable), subsidies, financing, cost of capital, degradation, and replacement.

Manufacturing yield: The fraction of manufactured cells or modules that operate as desired (i.e., within a desired tolerance of targeted performance parameters). All else equal, increasing manufacturing yield reduces module cost per watt.

Material complexity: The number of atoms in a unit cell, molecule, or other repeating unit of a material. Material complexity is related to the degree of disorder at the nanoscale. For current PV technologies, higher material complexity often translates to lower technological maturity, material intensity, processing temperatures, and processing complexity.

Material intensity: Amount of raw material required per unit of PV power output, in units of

mg/W_p or t/GW_p. Material intensity varies directly with active layer thickness and inversely with cell efficiency, materials utilization, and manufacturing yield.

Materials utilization (*U*): The fraction of original source material (feedstock) that ends up in a working solar cell. The remainder (1-*U*) is lost during processing. Efficient recycling of process waste can increase materials utilization.

Multijunction cell: A solar cell consisting of more than one charge-collecting junction. When stacked in order of decreasing bandgap, multiple junctions allow light of particular wavelength ranges to be absorbed and photovoltaic energy conversion to occur in the sub-cell that incurs minimal thermal losses for that wavelength range.

Open-circuit voltage (V_{OC}): The voltage measured across the terminals of a solar cell under illumination when no load is applied. The open-circuit voltage is fundamentally related to the balance between light current and recombination current, and is thus a primary measure of the quality of a solar cell. PV technologies with high open-circuit voltages (i.e., close to the material-dependent bandgap) typically exhibit low internal losses.

Performance ratio (PR): The ratio of the actual AC energy output [kWh/y] of a PV system to the output of an ideal system with the same nameplate capacity and no DC-to-AC conversion losses, under local insolation conditions and at 25ºC. Performance ratios are often reported for individual months or years and are helpful for identifying failure of system components. The quality factor (Q) is the same as the performance ratio.

Processing complexity: A qualitative measure of the difficulty of purifying raw materials and manufacturing cells and modules for a given PV technology. Technologies with high processing complexity may require substantial capital equipment investments, many discrete manufacturing steps, high material purity, high-temperature processing, and long process times. Processing complexity tends to vary inversely with material complexity.

Recombination: Undesirable loss of charge carriers within a solar cell. Radiative recombination results in emission of a photon and is the basis of light-emitting device (LED) operation, while non-radiative recombination results in energy loss as heat. Recombination rates are often increased by defects in bulk semiconducting material or at interfaces.

Roll-to-roll (R2R) processing: General term for high-throughput film deposition on flexible substrates (e.g., papers, plastics, and textiles) in the form of continuous rolls. Roll-to-roll processing may reduce thin-film PV processing costs per area substantially, although commercial demonstrations at large scale are currently limited.

Shockley-Queisser limit: Maximum theoretical power conversion efficiency, originally derived by Shockley and Queisser in 1961, for a solar cell consisting of a single *pn* junction. This limiting efficiency depends on the assumed solar spectrum (e.g., blackbody approximation, AM0 outside Earth's atmosphere, or AM1.5G at the surface). The Shockley-Queisser or detailed balance efficiency limit is 33.7% for a bandgap of 1.34 eV, under the AM1.5G spectrum without concentration at 300 K.[2,3] Multijunction cells can achieve efficiencies above this value.

Solar fraction: The fraction of global electricity demand satisfied by solar photovoltaics.

Specific power: The power output per unit weight of a PV cell or module, in units of W/g. Thin-film solar cells can achieve higher specific power than wafer-based cells based on active layer weight alone, but substrate weight often dominates the specific power of today's thin-film cells.

Life Cycle Carbon Intensity of PV

The carbon footprint of solar PV (in grams of CO_2-equivalent per kWh of electricity produced [g CO_2-eq/kWh]) depends on both the electricity generated and the greenhouse gases (GHGs) emitted throughout the PV life cycle. A full life cycle assessment (LCA) tracks the complete environmental burden of PV—including material and energy flows—from upstream processes (i.e., materials extraction and processing, module and system component manufacturing, transportation, and installation) through 20–30 years of operation to downstream processes (i.e., plant decommissioning, recycling, and waste disposal).[4-13]

The life cycle carbon intensity of PV is typically dominated by emissions from the energy consumed during materials extraction and component manufacturing.[4] Ignoring differences in manufacturing energy consumption and installed system performance with location, we can roughly estimate the relative impact of manufacturing location and deployment location on the carbon footprint of c-Si PV. For this example, we consider the United States and China as representative locations for PV manufacturing and deployment. We acknowledge that a proper life cycle calculation for PV considers many more factors than those described in the equations below.[14,15] However, we adopt a simplistic approximation below, to elucidate the principal parameters that often govern life cycle calculations.

Life cycle carbon intensity of PV ≈ "Levelized" carbon footprint of PV manufacturing

$$C_{\mathrm{PV}} \approx C \times E \times \left(\frac{1}{Y}\right)$$

$$\left[\frac{\mathrm{g\ CO_2\text{-}eq}}{\mathrm{kWh}}\right] = \left[\frac{\mathrm{g\ CO_2\text{-}eq}}{\mathrm{kWh}}\right] \times \left[\frac{\mathrm{kWh}}{\mathrm{W_p}}\right] \times \left[\frac{\mathrm{W_p}}{\mathrm{kWh}}\right]$$

where C_{PV} = life cycle carbon intensity of PV
C = carbon intensity of local electricity[16]
C_{US} = 610 g CO_2-eq/kWh
C_{China} = 1049 g CO_2-eq/kWh
E = energy required to manufacture 1 W_p of PV
Y = energy yield ($1/Y$ = W_p required to get 1 kWh of lifetime output)*

A 2012 LCA harmonization study by Hsu *et al.*[4] screened a broad range of published c-Si PV LCAs and adjusted their estimates of life cycle GHG emissions to correct for different values of input parameters, including insolation, module efficiency, performance ratio, and system lifetime†. The analyses referenced in that study were published between 2000 and 2009, and as a result rely primarily on data from PV manufacturers in Europe and in the U.S. For an annual insolation of 1,700 kWh/m^2/y (194 W/m^2 or 4.7 kWh/m^2/day)—corresponding to the average insolation in southern Europe—the study reports a median (harmonized) life cycle carbon

* As mentioned above, the energy yield of a PV system depends directly on local insolation and system performance. In this analysis, we assume that the system performance is unaffected by deployment location, and hence differences in energy yield can be attributed to differences in insolation.

† Hsu and colleagues report harmonized results based on an annual insolation of 1,700 kWh/m^2/y, a module efficiency of 13.2% (mc-Si) or 14.0% (sc-Si), a performance ratio of 0.75 (rooftop and building-integrated systems) or 0.80 (ground-mounted systems), and a system lifetime of 30 years.

intensity of 45 g CO_2-eq/kWh, with an interquartile range of 39–49 g CO_2-eq/kWh.

As shown in **Figure 2** in the main text, the average irradiance in the continental U.S. ranges from 135–245 W/m^2 (3.2–5.9 kWh/m^2/day). Correcting for differences in insolation gives an estimated range for the median carbon intensity of c-Si PV modules manufactured in the U.S. and deployed in the U.S.: **36–65 g CO_2-eq/kWh**. If the primary factor contributing to life cycle GHG emissions is the carbon intensity of electricity in the manufacturing location, we can scale the values above by the ratio of the average carbon intensities of electricity in China and in the U.S. ($\frac{C_{\text{China}}}{C_{\text{US}}} = \frac{1049}{610}$) to estimate the carbon intensity of PV modules manufactured in China and deployed in the U.S.: **61–111 g CO_2-eq/kWh**.

The average irradiance in China ranges from 125–265 W/m^2 (3.0–6.4 kWh/m^2/day). Performing the same adjustments as before, we calculate the carbon intensity of PV manufactured in either the U.S. or China, and deployed in China. The results are listed below.

*Carbon intensity of PV modules manufactured in **U.S.** and deployed in **U.S.***

$$C_{\text{PV,US,US}} \approx C_{\text{US}} \times E \times \left(\frac{1}{Y_{US}}\right) \approx \textbf{36–65 g CO}_2\textbf{-eq/kWh}$$

*Carbon intensity of PV modules manufactured in **China** and deployed in **U.S.***

$$C_{\text{PV,China,US}} \approx C_{\text{China}} \times E \times \left(\frac{1}{Y_{US}}\right) \approx \textbf{61–111 g CO}_2\textbf{-eq/kWh}$$

*Carbon intensity of PV modules manufactured in **U.S.** and deployed in **China***

$$C_{\text{PV,US,China}} \approx C_{\text{US}} \times E \times \left(\frac{1}{Y_{China}}\right) \approx \textbf{33–70 g CO}_2\textbf{-eq/kWh}$$

*Carbon intensity of PV modules manufactured in **China** and deployed in **China***

$$C_{\text{PV,China,China}} \approx C_{\text{China}} \times E \times \left(\frac{1}{Y_{China}}\right) \approx \textbf{57–120 g CO}_2\textbf{-eq/kWh}$$

All of these ranges are much lower than the typical carbon intensities of natural gas (~500 g CO_2-eq/kWh) and coal (~1000 g CO_2-eq/kWh).[17] So PV electricity is cleaner than fossil fuel-based electricity from an emissions perspective, regardless of where the modules are manufactured and deployed. But the deployment location still matters: Deploying PV in China avoids more emissions than deploying PV in the United States, due to the high carbon intensity of electricity in China today.

*Avoided emissions with PV manufactured in **U.S.** and deployed in **China***

$C_{\text{China}} - C_{\text{PV,US,China}}$ = 1049 – (33 to 70) = **979–1016 g CO_2-eq/kWh** (best case)

*Avoided emissions with PV manufactured in **China** and deployed in **China***

$C_{\text{China}} - C_{\text{PV,China,China}}$ = 1049 – (57 to 120) = **929–992 g CO_2-eq/kWh**

*Avoided emissions with PV manufactured in **U.S.** and deployed in **U.S.***

$C_{\text{US}} - C_{\text{PV,US,US}}$ = 610 – (36 to 65) = **545–574 g CO_2-eq/kWh**

*Avoided emissions with PV manufactured in **China** and deployed in **U.S.***

$C_{US} - C_{PV,China,US}$ = 610 – (61 to 111) = **499–549 g CO_2-eq/kWh** (worst case)

Thus if our goal is to reduce emissions, it is far less important **where the PV is made** (reduction of -13–87 g CO_2-eq/kWh if manufactured in U.S. instead of China) than **where it is used** (380–493 g CO_2-eq/kWh if deployed in China instead of U.S.), and most important **whether it is used at all** (499–1016 g CO_2-eq/kWh if deployed).

Basics of Solar Photovoltaic Energy Conversion

Introduction

In this primer, we describe the principles governing the conversion of light into electricity in photovoltaic (PV) devices. We begin by discussing the fundamentals of energy conversion, light, and electric power. We next introduce the concept of semiconductors, describing the electrical and optical properties that govern their interaction with light. We explain the concept of the diode as the fundamental functional unit of a PV device and describe the characterization and standard performance metrics of solar cells. Finally, we discuss how solar cells are used in PV modules, arrays, and systems. For a more complete explanation of the physical concepts described here, we point the interested reader toward a number of relevant textbooks.[18-24]

Energy and Power

Energy can be defined as the capacity of a system to perform work.[*] In the International System of units, energy is measured in units of *joules* (J); 1 J is roughly the amount of energy required to lift a can of soda 1 foot off the ground.[†] *Power* is the rate of flow of energy per unit time and is measured in units of *watts* (W), where 1 W is equal to an energy flow of 1 J/s. Energy can thus equivalently be expressed in units of *watt-hours* (Wh) or, more commonly in the electric power sector, *kilowatt-, megawatt-, gigawatt-,* or *terawatt-hours* (kWh, MWh, GWh, and TWh, respectively). A typical home in the United States utilizes electric power at an average rate of roughly 1.24 kW, corresponding to an energy usage of ~30 kWh per day.[25]

Energy cannot be created or destroyed, but it can be stored and converted between different forms.[‡] There are many different forms of energy: The chemical energy stored in carbon-carbon bonds in a piece of coal, the gravitational potential energy of elevated water in a dammed reservoir, and the radiant energy continually delivered to the Earth's surface by the Sun are all familiar examples. What are typically thought of as energy *generation* devices—coal-fired power plants, hydroelectric dams, or solar panels—are thus actually energy *conversion* devices.

Fig. S1 summarizes, in a simplified format, the forms of energy and processes of energy conversion relevant to electric power generation. Note that the only continuous input of energy to the Earth is the radiant energy of the Sun. Each energy conversion process, here denoted by labeled arrows, involves the irreversible conversion of some portion of the energy input to low-grade thermal energy (i.e., waste heat). Some of these conversion processes are more efficient than others; while turbines can convert only around 30–40% of the thermal energy from burning coal into kinetic energy, generators can convert over 90% of the kinetic energy of a spinning turbine into electrical energy. Photovoltaics are unique in their ability to directly convert radiant solar energy to electrical energy, and by eliminating the relatively inefficient processes of

[*] We refer to *work* as it is used in physics; that is, as a measure of the force applied on a point in motion over a displacement in position, for the component of the force in the direction of that motion.

[†] Much more energy is contained *within* the can of soda; one joule is roughly the amount of extractable dietary energy contained in one-hundredth of a drop of soda.

[‡] Einstein's famous "$E=mc^2$" equation implies that mass and energy are equivalent properties and represent the same physical quantity—not that energy can be "created" from matter.

photosynthesis (0.5–2% efficient)[26] and thermal-to-kinetic-energy conversion, they represent the most direct and efficient use of Earth's primary energy input—sunlight.

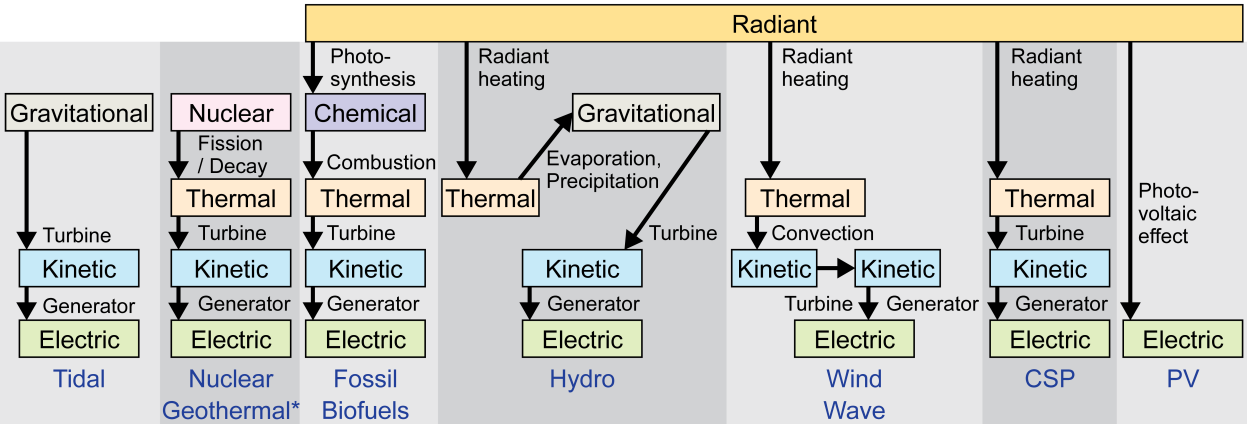

Fig. S1*: Relevant forms of energy (colored boxes) and energy conversion processes (labeled arrows) for the production of electric power. Note that gravitational, nuclear, and chemical energy all represent energy that can be stored for long periods of time with high efficiency; direct storage of thermal, kinetic, or electric energy is much less efficient. Radiant energy from the Sun is the only external energy input to the Earth system.*[*]

We next describe the properties of light (radiant power) and electricity (electric power)—the input and output of PV devices, respectively.

Light

Light refers to a specific type of *electromagnetic radiation* (EM) that is visible to the human eye. Electromagnetic radiation is comprised of alternating electric and magnetic fields that oscillate with a given *frequency* and *wavelength* and propagate in a straight line. **Fig. S2** graphically represents the EM spectrum. Visible light is typically characterized as EM radiation with a wavelength between 400 and 750 nanometers (nm);[†] as shown in the figure, we perceive light of different wavelengths as different colors. This range represents a small fraction of a spectrum that stretches over many orders of magnitude in wavelength (and frequency), from gamma and X rays, through ultraviolet, visible, and infrared radiation, to microwaves and radio waves.

The fundamental quantized unit (or quantum) of light is the *photon*, which represents the smallest isolable packet of EM radiation of a given wavelength. The energy content of a photon is proportional to its frequency and inversely proportional to its wavelength, and the power delivered by a light source to an absorbing surface is equal to the flux, or rate of flow, of photons absorbed by that surface times the energy of each incident photon. Most of the sun's emission spectrum lies between the ultraviolet and the infrared. The power delivered by solar radiation to a surface pointing toward the Sun, located at the Earth's surface at noon, on a cloudless day and at a latitude representative of many of the world's major population centers, is roughly 1000

[*] The flow of geothermal energy from the Earth's interior to its surface results in roughly equal measure from leftover energy still being dissipated from the Earth's formation and from the nuclear decay of radioactive isotopes in the Earth's interior.[27]

[†] One nanometer is 10^{-9} m; a human hair is roughly 75,000 nm in diameter.[28]

W/m^2, typically known as 1 sun. The nature of sunlight and its interaction with the Earth and its atmosphere is described in detail in Ref. 29.

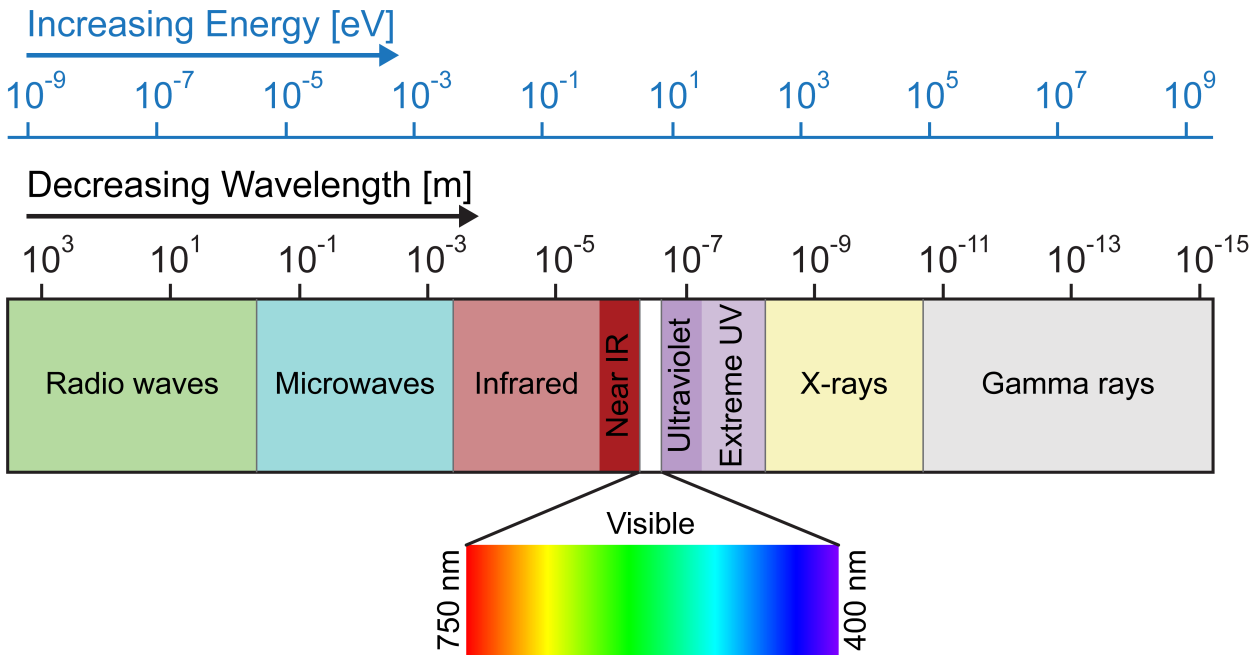

***Fig. S2**: Spectrum of electromagnetic radiation in units of energy (in electron-volts, eV, where 1 eV ≈ 1.6 × 10^{-19} J) and wavelength (in nm), with the visible range of light highlighted. Reprinted with permission from Ref. 30.*

Equation 1: Photon Energy
The energy of a photon E is given by

$$E = \frac{hc}{\lambda} = h\nu$$

where h is Planck's constant (~6.63 × 10^{-34} J-s), c is the speed of light in vacuum (299,792,458 m/s), λ is the photon wavelength, and ν is the photon frequency.

Electricity and Electric Power

Electricity is characterized by *voltage* and *current*. Current, measured in *amperes* or *amps* (A), corresponds to the rate of flow of charge; if we imagine electricity flowing through a wire in analogy to water flowing through a pipe, current is the rate of flow of the water. Voltage, measured in *volts* (V), corresponds to the electric potential energy difference, per unit charge, between two points. In our analogy of water flow, the voltage between two points corresponds to the pressure or height difference between those points; it is the driving force behind the flow. The electrical *resistance* of a sample of material, measured in *ohms* (Ω), is the ratio between the voltage applied to the sample and the current that flows through it; in our analogy, the resistance would be inversely proportional to the diameter of the pipe through which the water flows. Electric power is equal to the product of voltage and current.

Equation 2: Ohm's Law
Current I, voltage V, and electrical resistance R are related by Ohm's Law:

$$V = IR$$

We now describe the properties of charge carriers within electronic materials and explain how these materials can be used to fabricate solar cells.

Electronic Materials

A typical solid such as silicon contains roughly 7×10^{23} electrons/cm^3 of material, where an *electron* is a subatomic particle with an electric charge, by definition, of -1 e.[*,†] These electrons occupy states of well-defined energy within the solid; much like water filling up a bucket, electrons minimize their energy by filling up the lowest-energy states (the deepest part of the bucket, or the most tightly-bound atomic energy states) first.

Electrons are one of two types of charge carriers in a solid; the other is the *hole*, which is simply the absence of an electron in a position where an electron would normally be found. If electrons are compared to drops of water, holes can be compared to bubbles below the water's surface. Since it carries an absence of negative charge while surrounded by a sea of negatively charged electrons,[‡] a hole can be treated as a carrier of positive charge, moving in the opposite direction from an electron under an applied electric field. The *electrical conductivity* of a material is proportional to the volume density [cm^{-3}] of mobile electrons and holes multiplied by their *drift mobility* [cm^2/(V-s)] in that material, defined as the ratio of a charge carrier's velocity to the magnitude of the electric field that drives its motion.

Equation 3: Electrical Conductivity
The electrical conductivity σ of a material is given by

$$\sigma = \sigma_{\mathrm{e}} + \sigma_{\mathrm{h}} = q(n\mu_{\mathrm{e}} + p\mu_{\mathrm{h}})$$

where σ_{e} and σ_{h} are the electron and hole conductivities, respectively; q is the charge of the electron; n and p are respectively the electron and hole densities; and μ_{e} and μ_{h} are respectively the electron and hole mobilities.

Electrons can be *excited* by the absorption of external energy in the form of light or heat. A single excitation generates both an electron and a hole; the excited electron transfers to a higher-energy state and leaves a hole in its previous state. In a typical solid at room temperature, heat is manifested as minute vibrations in the atoms that make up the solid. For electrons, this heat behaves like a continuous spectrum of low-energy excitations, inducing small ripples on the surface of the energetic sea of electrons.

---

[*] A charge of "1 e" is equivalent to ~1.6×10^{-19} A-s, or the amount of charge that flows past a point when a current of 1 A is allowed to flow for ~1.6×10^{-19} s.

[†] An electron-volt (eV) can also be defined as the energy gained by an electron as it passes through a voltage difference of 1 V.

[‡] The negative charge of each electron is balanced by a positive charge in the nucleus of the atom from which the electron originates, such that the entire solid carries no net charge.

Like vibrational modes on a guitar string, only certain electron energies are allowed within a material. In a single atom or molecule, these energies exist as discrete, isolated energy states; in extended many-atom solids, these discrete states are smeared out into broad *energy bands*. In pure materials, electrons can only reside at energies within these bands; they cannot occupy energies between bands, where there are no electronic states. The electronic properties of a material are determined to a large extent by the shapes of these bands and the extent to which they are filled with electrons. The highest-energy band that is completely filled with electrons is called the *valence band*; the next-higher band is called the *conduction band*.

As shown in **Fig. S3**, the three major classes of electronic materials—*metals*, *insulators*, and *semiconductors*—are characterized by distinct energy band arrangements. *Metals* contain an incompletely filled energy band, allowing electrons at the energetic surface of the filled states to move (much like waves in a partially-filled container of water). *Insulators* contain completely filled bands separated by a large energy *bandgap*. This bandgap in insulators is too wide to allow significant excitation of electrons across the gap by heat (at typical operating temperatures) or visible photons. Because the valence band of insulators is completely filled with electrons (with no mobile holes) and the conduction band is completely empty of electrons, no charge carriers are available to flow under an applied electric field, making these materials electrically resistive. *Semiconductors* are intermediate between metals and insulators; they exhibit a bandgap that is small enough for electrons to be excited across it by heat or visible photons. Most importantly, semiconductors can be *doped* (intentionally or unintentionally) with minute quantities of foreign atoms that donate excess electrons or holes to the rest of the solid. Doping allows the density of free charge carriers and thus the conductivity of the material to be controlled over many orders of magnitude.

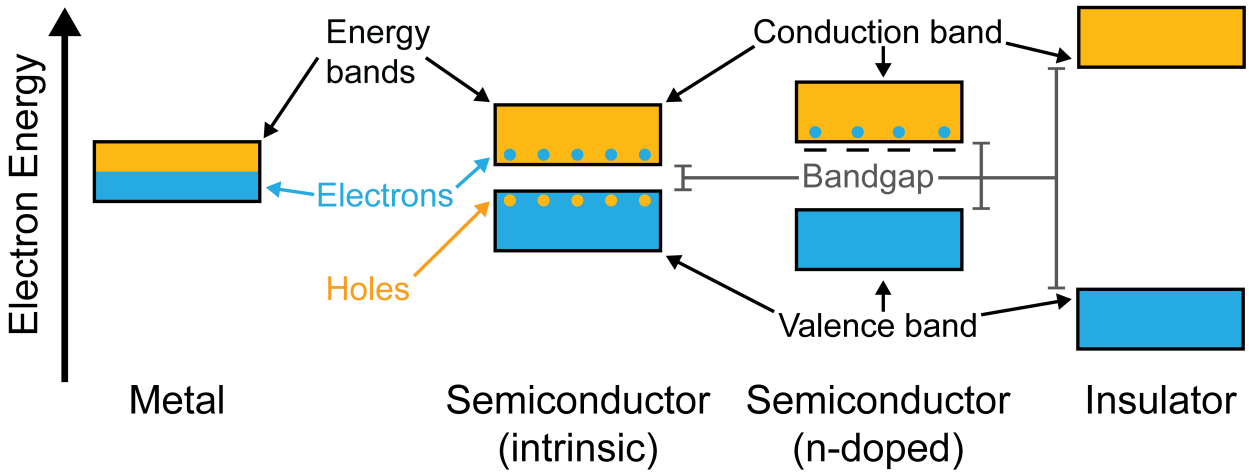

***Fig. S3**: Schematic electronic band structure of metals, semiconductors, and insulators.*

***Table 1**: Bandgaps of various materials. Common solar cell materials are highlighted in blue; insulators are highlighted in green.*[20,22,31-33]

Material	Bandgap [eV]
Metals	0
PbS (lead sulfide)	0.4
Si (silicon)	1.1
CdTe (cadmium telluride)	1.4
CIGS (copper indium gallium diselenide)	1.0–1.7
C (diamond)	5.5
SiO_2 (silica glass)	~9
LiF (lithium fluoride)	13.6

pn-Junction Diodes and Solar Cells

The fundamental functional unit of a solar cell is a *pn-junction diode*, which forms at the interface between two semiconductors: one doped with an excess of electron-donating impurities (an *n-type* semiconductor, so named for the excess of free *n*egatively-charged electrons), and one doped with an excess of hole-donating impurities (a *p-type* semiconductor, so named for the excess of free *p*ositively-charged holes). **Fig. S4** illustrates the fundamentals of the *pn*-junction diode. When an *n*-type and *p*-type material are put in contact, free electrons from the *n*-type side and free holes from the *p*-type side diffuse across the interface, cancelling each other out (the electrons "fill in" the holes). This elimination of the free carriers near the interface uncovers the fixed charges of the dopants that originally balanced the charge of the free electrons and holes, generating a built-in electric field in the interface region that prevents further diffusion. This field corresponds to a built-in voltage between the *n*-type and *p*-type sides of the junction.

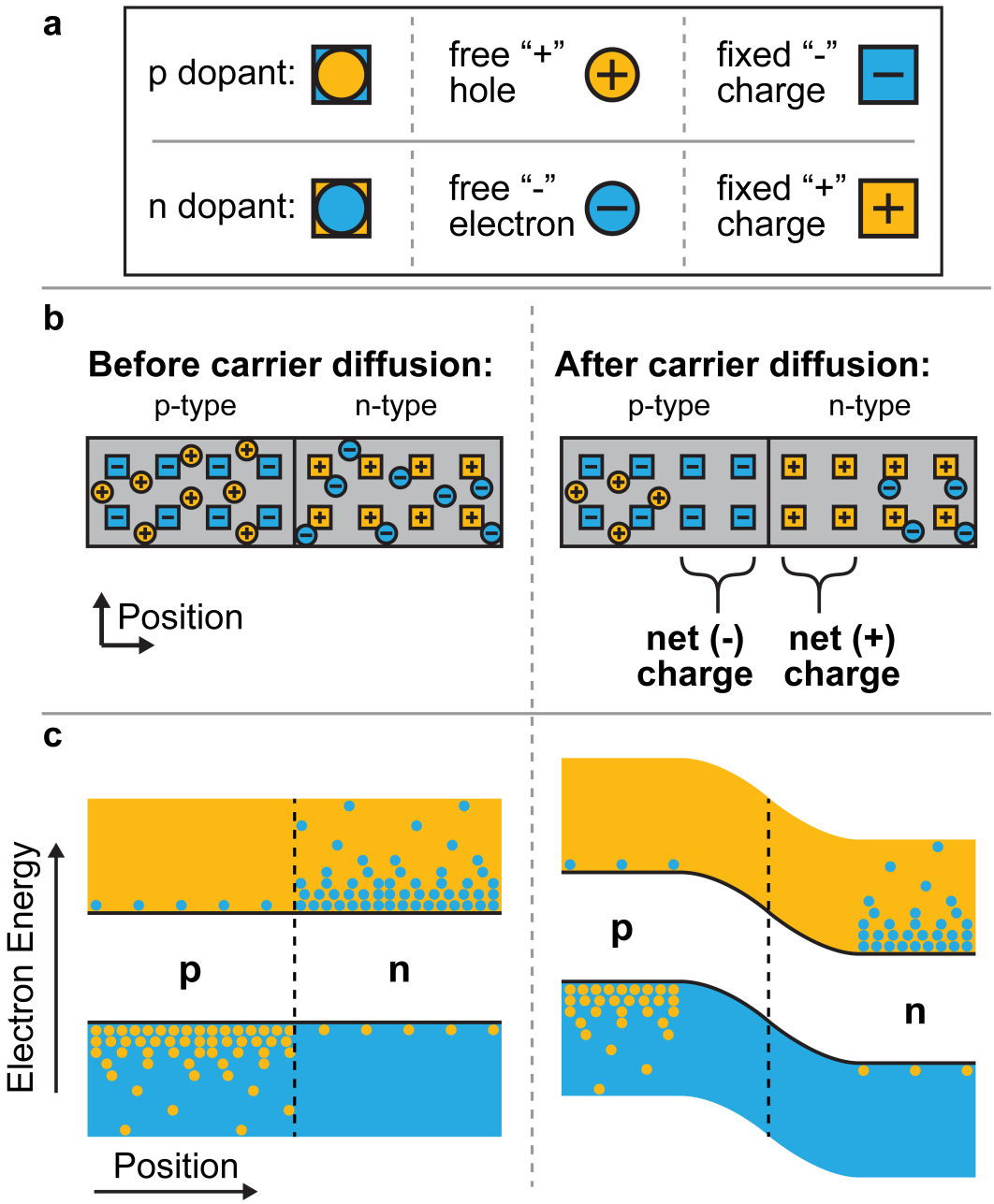

***Fig. S4**: Physical structure and electric properties of a pn-junction diode before and after diffusion of charge carriers across the junction interface.*

The diode acts as a one-way valve for charge carriers, as shown in **Fig. S5**. If a positive voltage is applied to the *p*-type side of the junction (forward bias), the built-in field is reduced, and large numbers of carriers can diffuse across the interface, generating a large current. If a negative voltage is applied to the *p*-type side (reverse bias), the built-in field is strengthened, diffusion remains unfavorable, and the current remains low. The current flow in a representative diode at different applied voltage levels is shown by the curve labeled "dark" in **Fig. S6**a: The current increases exponentially under positive voltage, but remains small under negative voltage.

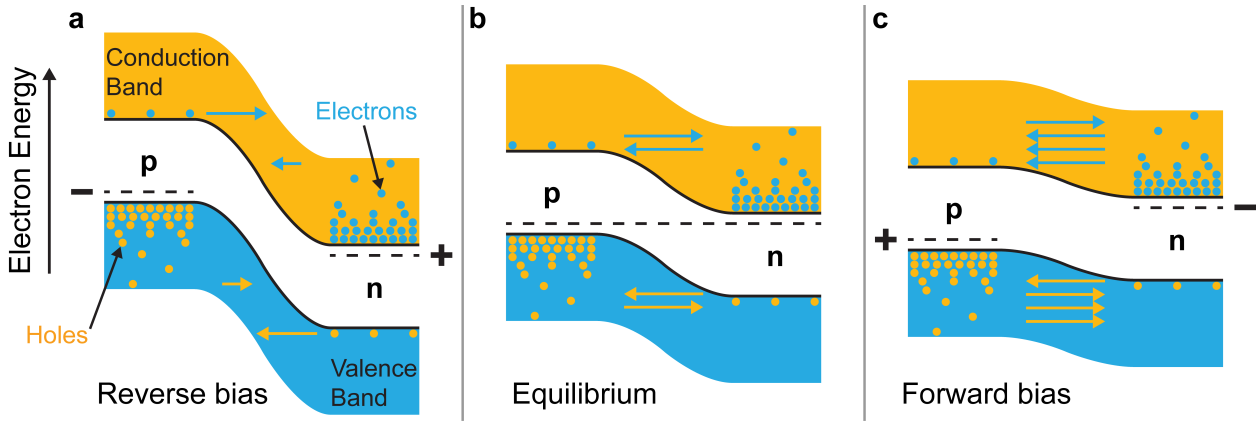

***Fig. S5**: Energy band diagram during operation of a pn-junction diode in the dark, showing (a) reverse bias, (b) equilibrium, and (c) forward bias conditions. Blue and orange arrows represent flux of electrons and holes, respectively.*

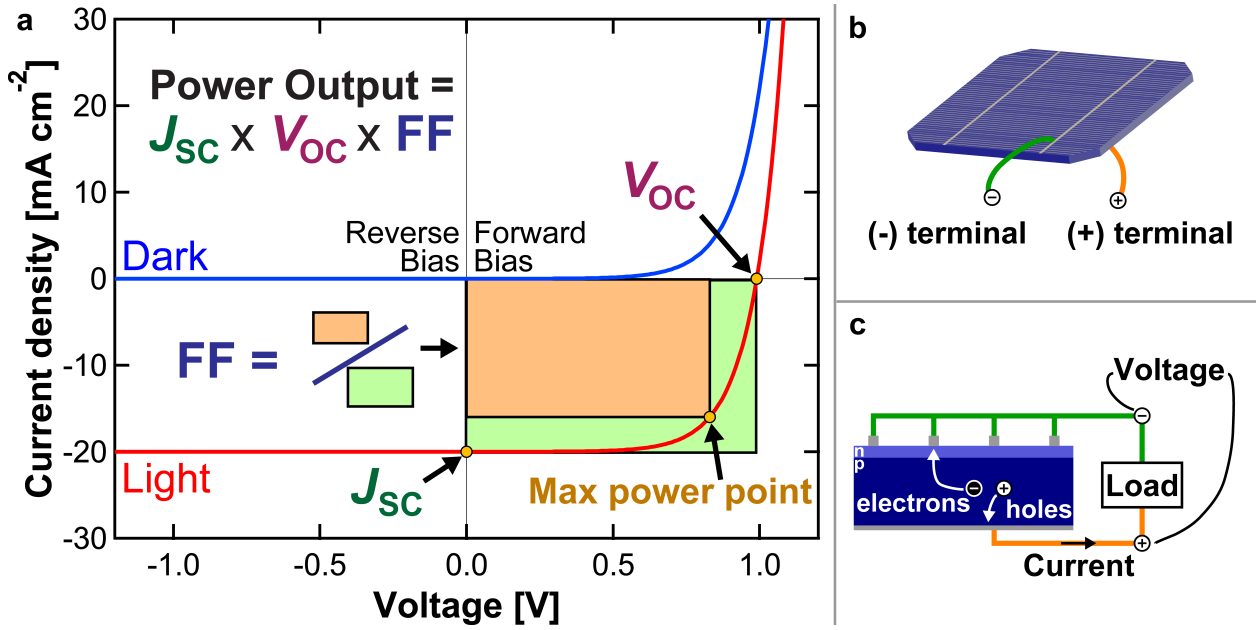

***Fig. S6**: (a) Representative current-voltage characteristics of a solar cell in the dark (blue curve) and under illumination (red curve). The short-circuit current density (J_{SC}), open-circuit voltage (V_{OC}), and fill factor (FF) are indicated; the physical significance of these metrics is described in the text. Since the current output of an illuminated solar cell is proportional to its illuminated surface area, the current density (current divided by area) normalizes for different cell sizes. Voltage and current are measured between the positive and negative terminals of the solar cell (b, c).*

A solar cell is simply a diode that can generate free electrons and holes through the absorption of light, as depicted in **Fig. S7**a. These free charge carriers are separated under the built-in electric field of the diode, generating photocurrent. Since the generation of photocurrent is roughly independent of the voltage across the solar cell, the "light" curve in **Fig. S6** is vertically offset by

a constant amount from the "dark" curve. The current is correlated with the number of carriers generated, which depends upon the absorption properties of the semiconductor and its efficiency in turning absorbed photons into extractable charge carriers (this efficiency, known as the *external quantum efficiency (EQE)*, is described in more detail below). The voltage is correlated with the strength of the built-in electric field of the diode.

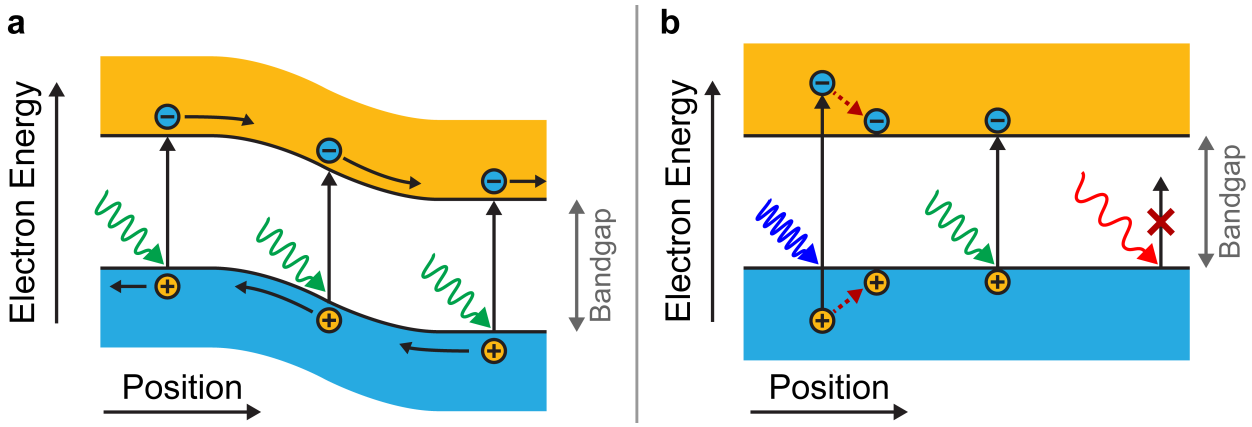

***Fig. S7**: (a) Operation of a solar cell under illumination, showing excitation of electrons and holes by light, followed by charge carrier separation under the built-in electric field. The conduction band and holes are shown in orange; the valence band and electrons are shown in blue. (b) Interaction of light of various wavelengths with a light-absorbing semiconductor. Short-wavelength photons of energy higher than the bandgap (here depicted as blue wavy arrows) generate excited electron-hole pairs with net energy greater than the bandgap, but the electron and hole quickly lose their excess energy and "relax" to the bottom of the conduction band (for electrons) and top of the valence band (for holes). Long-wavelength photons of energy lower than the bandgap (here depicted as red wavy arrows) are not absorbed and do not generate free electron-hole pairs.*

Fig. S6 illustrates the current-voltage output of a representative solar cell both in the dark (blue curve, acting as a simple diode) and under illumination (red curve), with key operational parameters identified. If the two terminals of an illuminated solar cell are left open (i.e., not connected to each other by a conductive path) and no current is allowed to flow, the voltage measured between them is the *open-circuit voltage* (V_{OC}). If the two terminals are shorted together by a highly conductive pathway (like a copper wire) and thus held at the same voltage, the current flowing through that pathway—divided by the cell area—is the *short-circuit current density* (J_{SC}).

Equation 4: Current-Voltage Characteristics of a Solar Cell
The current density output from a solar cell, J_{PV}, as a function of voltage is given by

$$J_{PV} = J_0 \left(e^{\frac{qV}{k_B T}} - 1 \right) - J_{SC}$$

where J_0 is the reverse saturation current density [mA/cm^2], q is the charge of the electron, V is the applied voltage, k_B is the Boltzmann constant (1.38×10^{-23} J/K), T is the temperature [K], and J_{SC} is the short-circuit current density [mA/cm^2]. With J_{SC} set to zero, this equation represents the output of a simple diode.

The voltage across the terminals of an operating solar cell can range between zero and V_{OC}; the current output stays roughly constant over much of this range, until the voltage approaches V_{OC}. The power output at a given voltage is equal to the product of the current and the voltage and will reach a maximum near the apparent "shoulder" in the current-voltage curve (as depicted by the orange rectangle in **Fig. S6**). The ratio between the power output per area at this *maximum power point* and the product of the J_{SC} and V_{OC} is the *fill factor*, which corresponds to the "squareness" of the illuminated current-voltage curve. The *power conversion efficiency (PCE)* is equal to the product of the short-circuit current density, open-circuit voltage, and fill factor, divided by the power per area of the incident light source (usually measured under standard illumination conditions of 1000 W/m^2, as discussed above).

Solar Cell Efficiency

The current and voltage output of a solar cell cannot be simultaneously optimized. Since a solar cell can only absorb photons with energy greater than the bandgap, reducing the bandgap generally increases current. However, as depicted in **Fig. S7**b, electrons excited by photons with energy greater than the bandgap quickly dissipate their excess energy as wasted heat, ultimately settling at an energy equal to the bandgap. The bandgap energy is thus the maximum energy that can be extracted as electrical energy from each photon absorbed by the solar cell. Reducing the bandgap leads to smaller voltages, eventually counteracting the benefit of increased current. The broad emission spectrum of the sun thus limits our ability to harvest both the maximum number of photons and the maximum energy from each photon.

The maximum power conversion efficiency of a *single-junction* solar cell, under unconcentrated solar illumination and room-temperature operation, is roughly 33%, a quantity known as the *Shockley-Queisser Limit*.[2,3] This limit can be surpassed by *multijunction* solar cells that use a combination of materials of different bandgaps; these devices enable a greater fraction of the energy of each absorbed photon to be extracted as voltage and have demonstrated efficiencies up to 46% under concentrated sunlight. In an actual solar cell, the presence of defects and parasitic resistive losses decreases the efficiency to values below the theoretical limits.

As mentioned above, the external quantum efficiency of a solar cell is the efficiency with which individual photons of a given wavelength are converted to extractable charge carriers. **Fig. S8** shows the EQE spectra of world-record solar cells of various types, compared with the solar spectrum observed at the Earth's surface. A sharp cutoff in EQE is observed on the high-wavelength (low-energy) side of each spectrum at the bandgap of the absorbing material, as photons with energy less than the bandgap cannot be absorbed. The multiplicative product of the

EQE spectrum and the solar spectrum, integrated over all wavelengths, is proportional to the short-circuit current produced by the solar cell. Incomplete absorption of the incident light by the solar cell active material may result from light reflection and from absorption by non-current-generating materials within the cell. These absorption losses, along with parasitic resistances, decrease the EQE to below 100%.

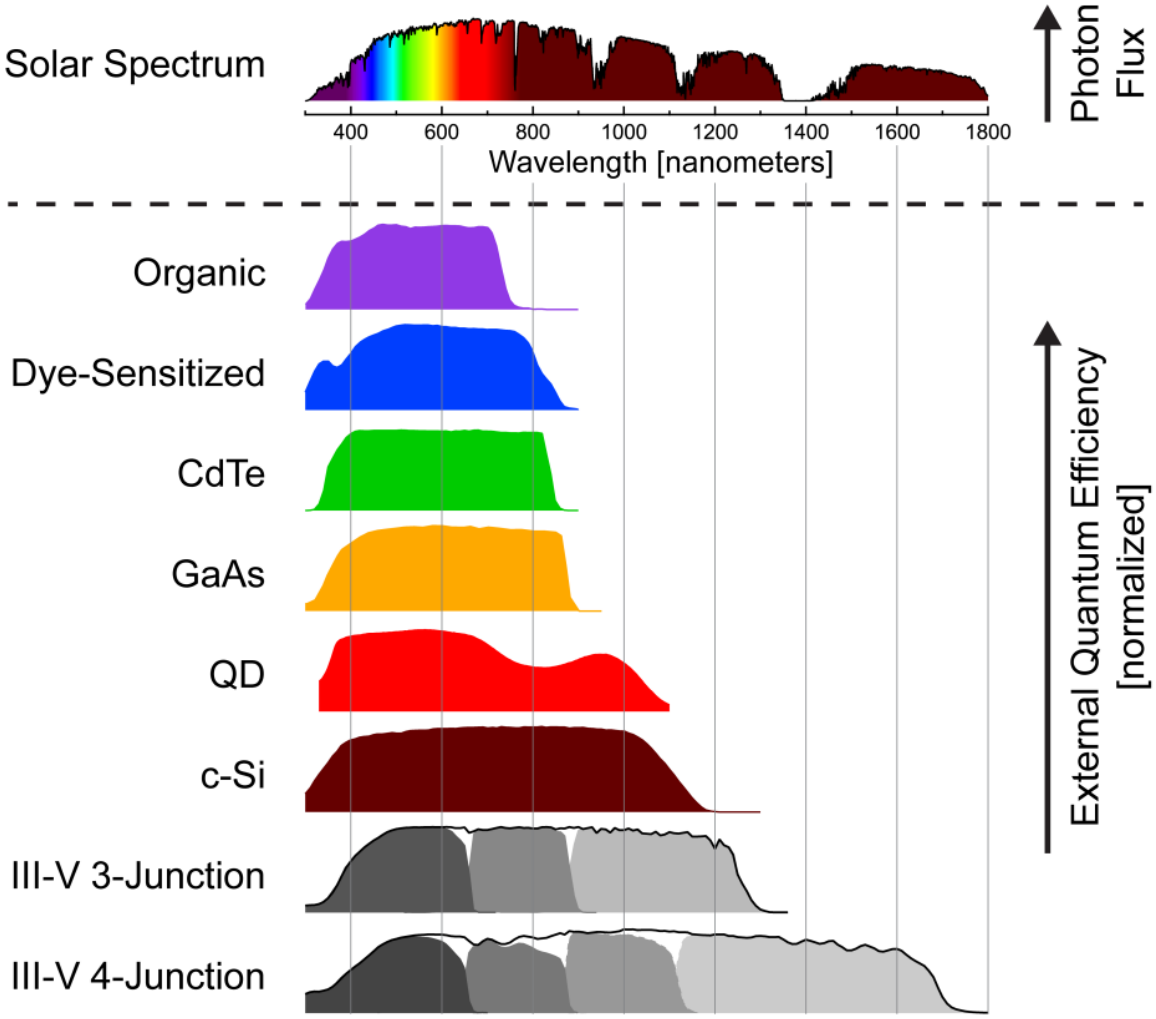

Fig. S8*: Solar photon flux at the Earth's surface as a function of wavelength, and normalized external quantum efficiency spectra for different solar cells.*[34-38] *The solar cell technologies listed here are described in more detail in the main text.*

Solar Cell Fabrication

A solar cell can be fabricated by one of two general methods: modification of a bulk wafer or additive deposition of thin films onto a substrate. The first approach, wafer modification, is used for conventional crystalline silicon cells and III-V multijunction cells. In this method, an extremely pure wafer of semiconductor is used as the starting material and dopants are introduced near the surface to create a *pn* junction. The wafer serves as both light absorber and substrate; charge carriers are generated within the wafer and extracted directly from the front

(top) and back (bottom) faces of the wafer by electrical contacts. The second approach, additive deposition, is used to make most thin-film solar cells. Here a separate substrate—a sheet of glass, plastic, or metal, which can be either rigid or flexible—serves as a mechanical support for the active cell. Light-absorbing films and electrical contacts are formed in a layer-by-layer process on the substrate by vapor- or solution-based deposition techniques such as thermal evaporation, chemical vapor deposition, spray coating, or screen printing. Different materials can be individually optimized for light absorption and charge transport, and additional layers are often introduced to enhance charge extraction.

Solar PV Arrays and Systems

A single 6" × 6" (15 cm × 15 cm) crystalline silicon solar cell generates a voltage of ~0.5–0.6 V and a power output of ~4–5 W under illumination with direct sunlight at an intensity of 1000 W/m^2. As shown in **Fig. S9**, individual cells are connected in *series* in a PV *module* or *panel* to increase their collective voltage output; a typical module contains 60 to 72 individual cells, generating a voltage of 30–48 V and a power output of 260–320 W. PV modules often incorporate additional materials, such as a glass sheet for mechanical support and protection, laminated encapsulation layers (commonly ethylene vinyl acetate, or EVA) for UV and moisture protection, a fluoropolymer backsheet for further environmental protection, and an aluminum frame for mounting (**Fig. S10**). Common module dimensions are 1 m × 1.5 m × 4 cm.

PV modules are typically connected in series to further increase their collective output voltage, or in *parallel* to increase their collective output current; such a collection of PV modules is often called a solar PV *array*. PV arrays can be stationary or can utilize solar tracking, whereby the modules are rotated throughout the day to point toward the sun, increasing the power output per panel. Some arrays—particularly those utilizing multijunction solar cells—use mirrors or lenses to concentrate sunlight onto the solar cells. Concentrating systems allow smaller solar cells to be used, but typically require accurate solar tracking to keep the concentrated sunlight focused onto the cells.

In addition to PV modules, a typical solar PV system also includes additional *balance-of-system* (BOS) components such as combiner boxes, inverters, transformers, racking, wiring, disconnects, and enclosures. Since most BOS components today vary with application but not with PV technology, we refer the reader to the literature on hardware[39] and non-hardware "soft"[40] BOS costs. In a grid-connected system, inverters and transformers convert the low-voltage *direct-current* (DC) output of a solar array into high-voltage *alternating-current* (AC) power that is fed into the electric grid. In an off-grid system, the DC output may be utilized directly, or batteries and charge controllers may be incorporated to store energy for later use.

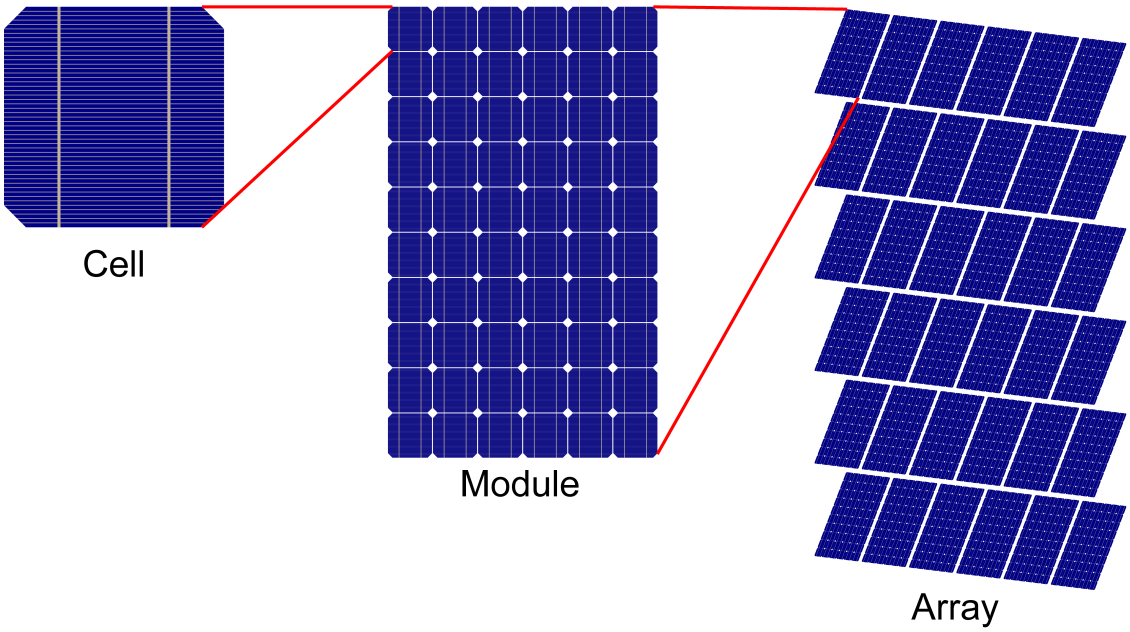

***Fig. S9**: Schematic representation of a solar cell, a solar PV module incorporating multiple cells, and a solar PV array incorporating multiple modules. Balance-of-system components such as racking, wiring, inverters, and transformers are not shown.*

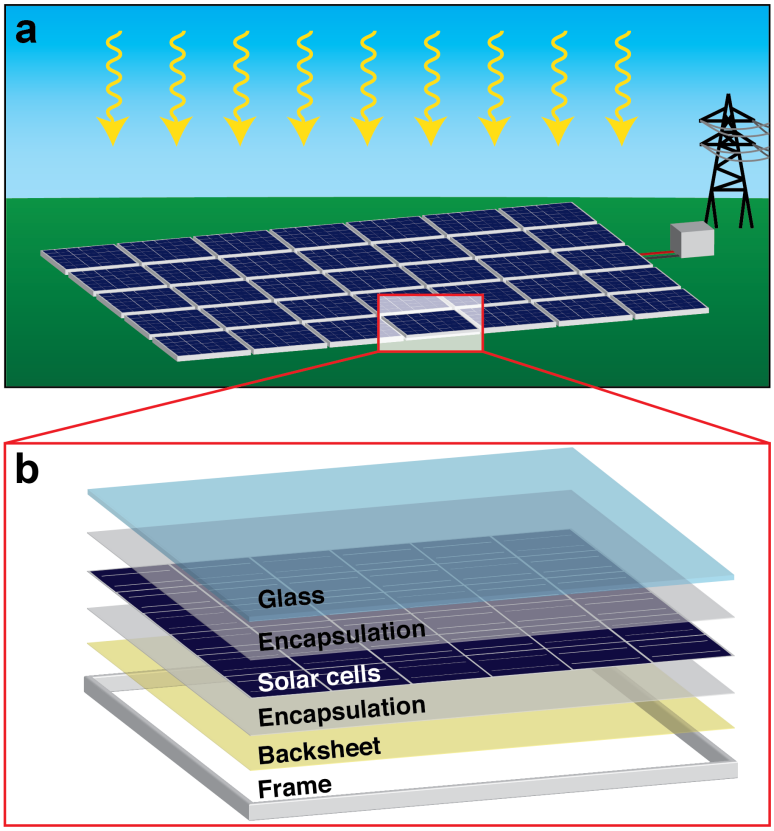

***Fig. S10**: (a) Illustration of grid-connected PV system. (b) Breakout view of PV module.*

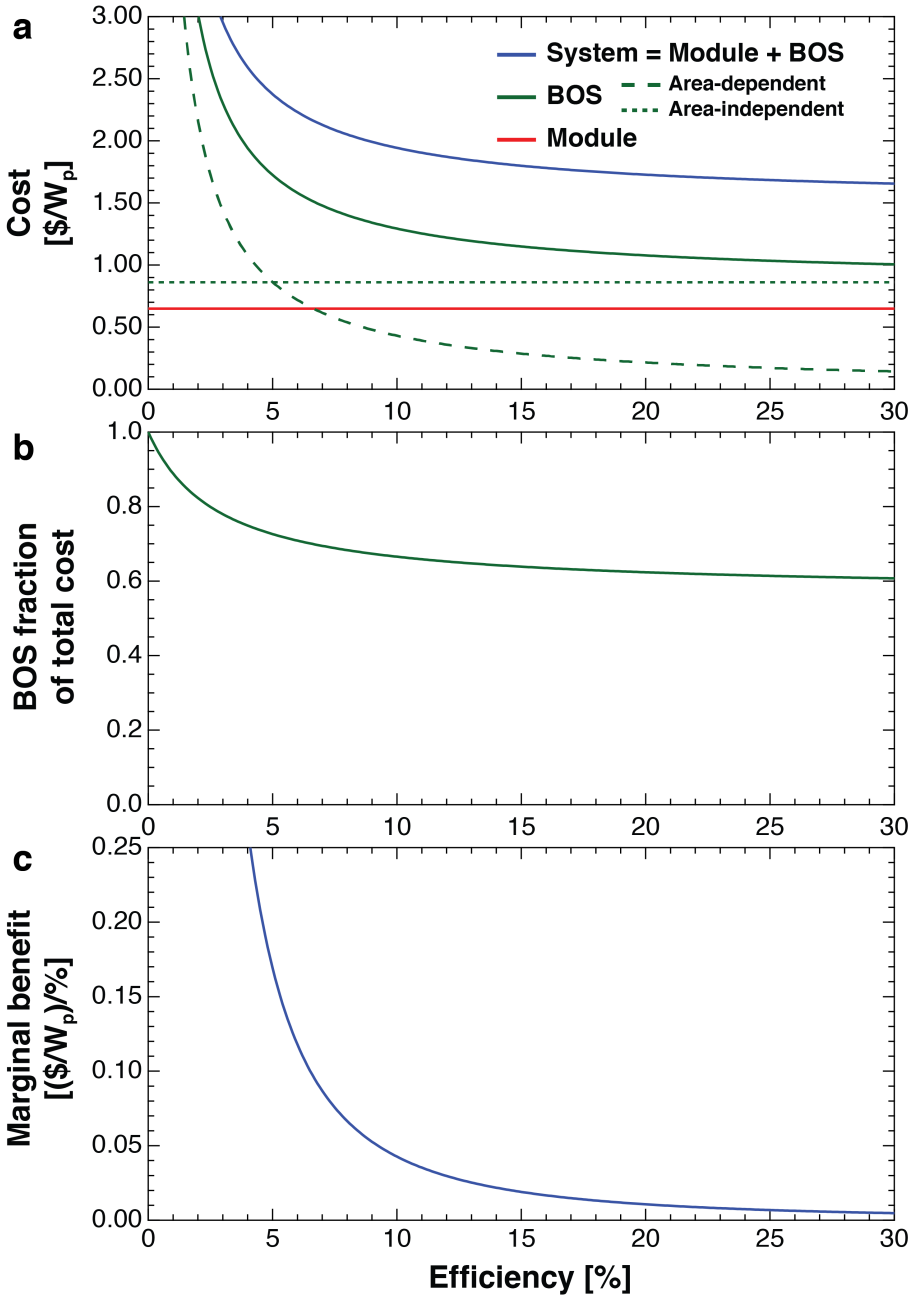

Fig. S11*: Effect of module efficiency on PV system cost. (a) Contribution of module and BOS to system costs. BOS cost components can be divided into two categories: area-dependent (e.g., land, materials and labor for wiring and mounting) and area-independent (e.g., inverters, permitting, interconnection, and taxes). One-quarter of BOS costs at 15% PCE are assumed to scale with area, consistent with estimates for a fixed-tilt utility-scale system.*[41] *At 15% PCE, modules constitute 36% of the total system cost of $1.80/W_p$.*[29] *A constant module price of $0.65/W_p$ is assumed.*[42] *(b) Higher module efficiencies reduce the importance of area-dependent and hence total BOS costs. At low efficiencies, the fraction of the system cost attributable to BOS approaches unity due to the larger system area required. (c) The marginal cost reduction from increasing PCE by a fixed quantity (e.g., one percentage point) decreases with increasing absolute efficiency.*

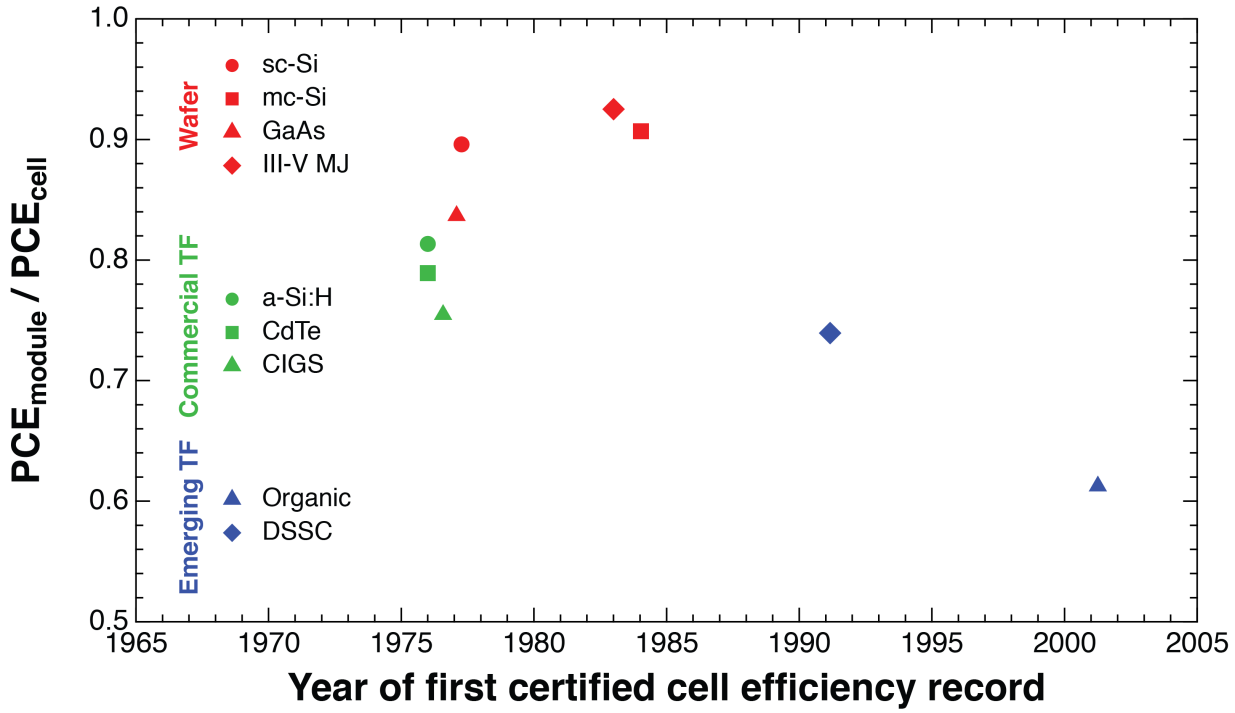

***Fig. S12**: Effect of development time on relative record efficiencies of cells and modules. Module efficiencies tend to be closer to cell efficiencies for older technologies. The time elapsed since the first NREL-recognized cell efficiency is used as a proxy for development time.[43,44] We note that this metric is an imperfect proxy, particularly for older technologies. The advent of some solar technologies predates their first certified efficiency measurement; for example, the first modern c-Si cell was demonstrated in 1954, while the first certification reported by NREL occurred in 1977. Early technologies are thus shifted to the right of their true values. Correcting for this effect would likely only strengthen the observed trend. Some emerging thin-film technologies (CZTS, perovskites, and QDPV) are omitted because few or no modules have been demonstrated.*

References

[1] *CRC Handbook of Chemistry and Physics, 95th Edition, 2014-15*, Taylor and Francis, 2014, www.hbcpnetbase.com (accessed 18 September 2014).
[2] W. Shockley and H. J. Queisser, *J. Appl. Phys.*, 1961, **32**, 510–519.
[3] M. C. Hanna and A. J. Nozik, *J. Appl. Phys.*, 2006, **100**, 074510.
[4] D. D. Hsu, P. O'Donoughue, V. Fthenakis, G. A. Heath, H. C. Kim, P. Sawyer, J.-K. Choi and D. E. Turney, *J. Ind. Ecol.*, 2012, **16**, S122–S135.
[5] H. C. Kim, V. Fthenakis, J.-K. Choi and D. E. Turney, *J. Ind. Ecol.*, 2012, **16**, S110–S121.
[6] V. M. Fthenakis, *Renewable Sustainable Energy Rev*., 2004, **8**, 303–334.
[7] V. Fthenakis, *Renewable Sustainable Energy Rev.*, 2009, **13**, 2746-2750.
[8] V. Fthenakis, *How Long Does it Take for Photovoltaics To Produce the Energy Used?*, PE Magazine, 2012, pp. 16-17.
[9] V. M. Fthenakis, *Energy Policy*, 2000, **28**, 1051-1058.
[10] E. A. Alsema, *Prog. Photovolt: Res. Appl.*, 2000, **8**, 17-25.
[11] V. M. Fthenakis and H. C. Kim, *Sol. Energy*, 2011, **85**, 1609-1628.
[12] M. Raugei, S. Bargigli and S. Ulgiati, *Energy*, 2007, **32**, 1310-1318.
[13] V. M. Fthenakis, H. C. Kim and E. Alsema, *Environ. Sci. Technol.*, 2008, **42**, 2168-2174.
[14] S. Pacca, D. Sivaraman and G. A. Keoleian, *Energy Policy*, 2007, **35**, 3316-3326.
[15] K. Kawajiri and Y. Genchi, *Environ. Sci. Technol.*, 2012, **46**, 7415-7421.
[16] *Safeguarding the Ozone Layer and the Global Climate System*, Intergovernmental Panel on Climate Change, 2005, https://www.ipcc.ch/pdf/special-reports/sroc/Tables/t0305.pdf (accessed 26 January 2015).
[17] J. E. Trancik and D. Cross-Call, *Environ. Sci. Technol.*, 2013, **47**, 6673-6680.
[18] R. Resnick, D. Halliday and K. S. Krane, *Physics*, John Wiley & Sons, Inc., Hoboken, NJ, 5th edn., 2002.
[19] D. J. Griffiths, *Introduction to Electrodynamics*, Prentice-Hall, Inc., Upper Saddle River, NJ, 3rd edn., 1999.
[20] C. Kittel, *Introduction to Solid State Physics*, John Wiley & Sons, Inc., Hoboken, NJ, 8th edn., 2005.
[21] N. W. Ashcroft and N. D. Mermin, *Solid State Physics*, Brooks/Cole, Belmont, CA, 1976.
[22] B. L. Anderson and R. L. Anderson, *Fundamentals of Semiconductor Devices*, McGraw-Hill, New York, 2005.
[23] J. Nelson, *The Physics of Solar Cells*, Imperial College Press, London, 2003.
[24] P. Würfel, *Physics of Solar Cells*, Wiley-VCH, Weinheim, 2009.
[25] *Frequently Asked Questions*, U.S. Energy Information Administration, 2014, http://www.eia.gov/tools/faqs/faq.cfm?id=97&t=3 (accessed 22 January 2015).
[26] D. J. C. MacKay, *Sustainable Energy - Without the Hot Air*, UIT Cambridge Ltd., Cambridge, 2009.
[27] T. Lay, J. Hernlund, J. and B. A. Buffett, *Nat. Geosci.,* 2008, **1**, 25–32.
[28] G. T. Smith, *Industrial Metrology*, Springer, London, 2002, p. 253.
[29] *MIT Future of Solar Energy Study*, in press.
[30] R. L. Jaffe and W. Taylor, *The Physics of Energy*, to be published by Cambridge University Press.
[31] S. H. Wei and A. Zunger, *J. Appl. Phys.*, 1995, **78**, 3846–3856.

[32] C. D. Clark, P. J. Dean and P. V. Harris, *Proc. R. Soc. Lond. A.*, 1964, **277**, 312-329.
[33] D. M. Roessler and W. C. Walker, *J. Phys. Chem. Solids*, 1967, **28**, 1507–1515.
[34] M. A. Green, K. Emery, Y. Hishikawa, W. Warta and E. D. Dunlop, 2012, **20**, 12–20.
[35] M. A. Green, K. Emery, Y. Hishikawa, W. Warta and E. D. Dunlop, 2012, **20**, 606-614.
[36] M. A. Green, K. Emery, Y. Hishikawa, W. Warta and E. D. Dunlop, 2013, **21**, 1-11.
[37] M. A. Green, K. Emery, Y. Hishikawa, W. Warta and E. D. Dunlop, 2013, **21**, 827-837.
[38] C. M. Chuang, P. R. Brown, V. Bulović and M. G. Bawendi, *Nat. Mater.*, 2014, **13**, 796-801.
[39] L. Bony, S. Doig, C. Hart, E. Maurer and S. Newman, *Achieving Low-Cost Solar PV: Industry Workshop Recommendations for Near-Term Balance of System Cost Reductions*, Rocky Mountain Institute, 2010, http://www.rmi.org/Content/Files/BOSReport.pdf (accessed 18 September 2014).
[40] B. Friedman, K. Ardani, D. Feldman, R. Citron, R. Margolis and J. Zuboy, *Benchmarking Non-Hardware Balance-of-System (Soft) Costs for U.S. Photovoltaic Systems, Using a Bottom-Up Approach and Installer Survey – Second Edition*, 2014, http://www.nrel.gov/docs/fy14osti/60412.pdf (accessed 18 September 2014).
[41] A. Goodrich, T. James and M. Woodhouse, *Residential, Commercial, and Utility-Scale Photovoltaic (PV) System Prices in the United States: Current Drivers and Cost-Reduction Opportunities*, 2012, http://www.nrel.gov/docs/fy12osti/53347.pdf (accessed 3 February 2015).
[42] *Module Price Index*, pvXchange, 2015, http://www.pvxchange.com/priceindex/Default.aspx?langTag=en-GB (accessed 3 February 2015).
[43] *Best Research-Cell Efficiencies (rev. 12-18-2014)*, National Renewable Energy Laboratory, 2014, http://www.nrel.gov/ncpv/images/efficiency_chart.jpg (accessed 10 February 2015).
[44] M. A. Green, K. Emery, Y. Hishikawa, W. Warta and E. D. Dunlop, *Prog. Photovolt: Res. Appl.*, 2015, **23**, 1–9.